DESIGN OF SERIES-FED PRINTED SLOT ANTENNA ARRAYS EXCITED BY MICROSTRIP LINES

A THESIS SUBMITTED TO
THE GRADUATE SCHOOL OF NATURAL AND APPLIED SCIENCES
OF
MIDDLE EAST TECHNICAL UNIVERSITY

BY

MUSTAFA İNCEBACAK

IN PARTIAL FULFILLMENT OF THE REQUIREMENTS
FOR
THE DEGREE OF MASTER OF SCIENCE
IN
ELECTRICAL AND ELECTRONICS ENGINEERING

SEPTEMBER 2010

Approval of the thesis:

DESIGN OF SERIES-FED PRINTED SLOT ANTENNA ARRAYS EXCITED BY MICROSTRIP LINES

submitted by **MUSTAFA İNCEBACAK** in partial fulfillment of the requirements for the degree of **Master of Science in Electrical and Electronics Engineering Department, Middle East Technical University** by,

Prof. Dr. Canan Özgen ____________
Dean, Graduate School of **Natural and Applied Sciences**

Prof. Dr. İsmet Erkmen ____________
Head of Department, **Electrical and Electronics Engineering**

Assist Prof. Dr. Lale Alatan ____________
Supervisor, **Electrical and Electronics Engineering Dept., METU**

Examining Committee Members:

Prof. Dr. Altunkan Hızal ____________
Electrical and Electronics Engineering Dept., METU

Assist. Prof. Dr. Lale Alatan ____________
Electrical and Electronics Engineering Dept., METU

Assoc. Prof. Dr. Sencer Koç ____________
Electrical and Electronics Engineering Dept., METU

Assoc. Prof. Dr. Özlem Aydın Çivi ____________
Electrical and Electronics Engineering Dept., METU

Assoc. Prof. Dr. Vakur Behçet Ertürk ____________
Electrical and Electronics Engineering Dept., Bilkent University

Date: 03.09.2010

I hereby declare that all information in this document has been obtained and presented in accordance with academic rules and ethical conduct. I also declare that, as required by these rules and conduct, I have fully cited and referenced all material and results that are not original to this work.

Name, Last name : Mustafa İncebacak

Signature :

ABSTRACT

DESIGN OF SERIES-FED PRINTED SLOT ANTENNA ARRAYS EXCITED BY MICROSTRIP LINES

İncebacak, Mustafa
M.S., Department of Electrical and Electronics Engineering
Supervisor: Assist. Prof. Dr. Lale Alatan

September 2010, 54 pages

Series-fed printed slot antenna arrays excited by microstrip lines are low profile, easy to manufacture, low cost structures that found use in applications that doesn't require high power levels with having advantage of easy integration with microwave front-end circuitry. In this thesis, design and analysis of microstrip line fed slot antenna arrays are investigated. First an equivalent circuit model that ignores mutual coupling effects between slots is studied. A 6-element array is designed by using this equivalent circuit model. From the measurement and electromagnetic simulation results of this array, it is concluded that mutual coupling effects should be considered in order to achieve a successful design that meets the design specifications related to the main beam direction and sidelobe levels of the antenna. Next, an improved equivalent circuit model proposed for stripline fed slot antenna arrays is studied. It is observed that, the mutual coupling effects are incorporated into the equivalent model through the utilization of active impedance concept. Finally, the design equations proposed in the improved equivalent circuit model are derived for the microstrip line fed slot antenna array structure. To demonstrate the validity and the accuracy of the derived design equations, results obtained by the proposed analysis method are compared with simulation and measurement results. It is concluded that the proposed method successfully predicts the radiation pattern of the array by including the mutual coupling effects.

Keywords: Microstrip-Fed Slot Antenna, Linear Array, Mutual Coupling, Equivalent Circuit Model, Self Impedance, Active Impedance

ÖZ

MİKROŞERİT HAT İLE SERİ BESLENEN YARIK ANTEN DİZİLERİ TASARIMI

İncebacak, Mustafa

Yüksek Lisans, Elektrik ve Elektronik Mühendisliği Bölümü

Tez Yöneticisi: Yrd. Doç. Dr. Lale Alatan

Eylül 2010, 54 sayfa

Mikroşerit hat ile seri beslenen yarık anten dizileri, ince ve hafif yapıları, düşük maliyetli ve kolay üretimlerinin yanı sıra mikrodalga devrelerle kolay entegre edilebilmeleri sebebiyle yüksek güç gerektirmeyen uygulamalarda kullanım alanı bulmaktadır. Bu tezde, mikroşerit hat ile beslenen yarık dizilerinin tasarım ve analiz yöntemleri incelenmektedir. İlk olarak yarıklar arasındaki karşılıklı bağlaşımın etkisinin ihmal edildiği bir eşdeğer devre modeli incelenmiştir. Bu model kullanılarak 6 elemanlı bir dizi tasarlanmıştır. Bu dizinin elektromanyetik benzetimi ve ölçümünden elde edilen sonuçlara göre, ana hüzme ve yan hüzme seviyeleri açısından tasarım isterlerinin başarılı bir şekilde karşılanması için karşılıklı bağlaşım etkisinin tasarıma katılması gerektiği düşünülmüştür. Şerit hat ile beslenen yarık anten dizileri üzerinde yapılan çalışmalar incelendiğinde karşılıklı bağlaşım etkilerinin eşdeğer devre modeline, geliştirilen aktif empedans konsepti ile dahil edildiği görülmüştür. Sonuç olarak, bu eşdeğer devre modeli için verilen tasarım denklemleri mikroşerit hat ile beslenen yarık anten dizileri için çıkarılmıştır. Bulunan bu tasarım denklemlerinin geçerliliğinin ve doğruluğunun denenmesi için bu

denklemlerle yapılan analiz sonuçları benzetim ve ölçüm sonuçları ile karşılaştırılmıştır. Karşılıklı bağlaşım etkilerinin dahil edildiği bu analiz yöntemiyle dizilerin ışınım örüntülerinin başarılı bir şekilde tahmin edildiği sonucuna varılmıştır.

Anahtar Kelimeler: Mikroşerit Hat ile Beslenen Yarık Anten, Doğrusal Dizi, Karşılıklı Bağlaşım, Eşdeğer Devre Modeli, Öz Empedans, Aktif Empedans

To my family

ACKNOWLEDGMENTS

I would like to express my sincere gratitude to my advisor Dr. Lale Alatan for her valuable supervision, support and encouragement throughout this thesis study. Without her insight and persistent believe in research, this thesis wouldn’t have been possible.

I would like to thank ASELSAN Inc. for the facilities provided. I would also like to thank TUBİTAK for funding graduate scholarship.

I am thankful to Seçkin Şenlik for his valuable friendship and encouragement throughout my graduate study and also throughout university years.

Lastly, I would like to express my sincerest thanks to my family for their understanding and support during this work. Especially, I am grateful to my sister Adile to stand as an inspiring person for me throughout my education life.

TABLE OF CONTENTS

LIST OF TABLES

TABLES

LIST OF FIGURES

CHAPTER 1

INTRODUCTION

Slot antennas that are formed by cutting narrow rectangular slots on a conducting plate, found widespread use in various applications due to their simple structures that offer the advantage of easy manufacturing, low cost and high-volume mass production. Different feeding configurations can be used for the excitation of slot antennas. The first applied and the most simple feeding configuration is the center-fed two-wire line excitation, where a potential difference across the slot is established by connecting each conductor of a two-wire transmission line to opposite edges of the slot. However, when array configurations are considered, a distributed type of feed configuration is preferred, in order to avoid the manufacturing of separate feeding structures for the excitation of each slot. Hence, waveguides found to be a very suitable transmission line medium to feed slot antennas and slotted waveguide antenna arrays (SWGAs) are proposed [1] and studied in detail for different slot configurations [2]. After the introduction of planar slotted waveguide antenna arrays, they started to be an attractive alternative to reflector antennas due to their low profile structures. Consequently, SWGAs are widely used in radar systems, especially in those applications that have space limitations like airborne radars [3].

There are two types of SWGAs: resonant arrays and traveling wave arrays. In resonant type arrays, the array is terminated with a short or open circuit. Resonant arrays are generally fed from the center of the array and they exhibit radiation in broadside direction. On the other hand, traveling wave type arrays are formed by feeding the array from one side and terminating the other side with a matched load. The traveling wave array radiates at an off-broadside direction which is determined by the inter-element spacing.

The main disadvantage of SWGAs is their narrow bandwidth property in terms of radiation characteristics. Since they are series fed arrays, the phase shift between array elements vary with changing frequency. Consequently, with changing frequency the main beam starts to split for resonant type arrays, and the main beam tilts for traveling wave type arrays. To overcome this problem, dividing the array into sub-arrays and feeding each sub-array in parallel is proposed [4]. The sub-array method improves the bandwidth of the array with a cost of more complex and bulky feed network. It is thought that the problem associated with the design and manufacturing of complex feed networks could be solved by using printed transmission lines instead of waveguides. Therefore microstrip line fed slot antenna arrays are studied in this thesis. Although microstrip line fed arrays are also advantageous due to their easy integration with active/passive microwave front-end circuitry, it should be noted that their usage is limited to applications which do not require high power levels since the power handling capacity of microstrip lines is low.

Microstrip fed slot antennas are formed by printing narrow rectangular slots on the ground plane of a microstrip line. This slot discontinuity on the ground plane intersects the surface currents and some part of the power, confined in the microstrip line, radiates. The amount of power radiating from the slot is controlled by the amount of current cut by the slot and it is related with the position and dimensions of the slot. In the configuration investigated in this thesis, slots cross the microstrip line orthogonally and as they move away from microstrip line in orthogonal direction (off-center feeding) radiated power decreases. Cascaded series connection of slots forms the array and the desired radiation pattern can be obtained by adjusting the magnitude and the phase of the radiation from each slot.

Yoshimura [5] represents one of the early works on microstrip line fed slot antennas in literature. In this work, off-center fed slots are treated experimentally. Effect of slot offset on radiation resistance is investigated and it is reported that as offset increases, radiated power decreases. Das and Joshi proposed to evaluate the input impedance of microstrip line fed slot antennas from the power radiated by the slot and the discontinuity in the modal voltage of the microstrip line and they verified the validity of their approach experimentally [6]. Full-wave analysis of a slot that is placed orthogonally to the microstrip line has been reported by Pozar [7]. In this work, he carries out an analysis based on the reciprocity theorem and finds the equivalent circuit model representing the slot discontinuity as series impedance. To extract the value of the series impedance, he conducts a Method of Moments (MoM) solution using exact spectral domain Green's functions for a grounded dielectric slab. Series impedance model found in this work forms a basis for more complex network models [8]-[10] proposed for the fast computation of the input impedance of microstrip-fed slot antennas.

By using the network model of a single slot, series arrays of cascaded slots can be designed. In [11], Tulintseff uses an equivalent circuit model to analyze linear arrays where slots are modeled by a series impedance. This equivalent circuit approach is also used in designing arrays. However, it doesn't encounter for mutual coupling between slots, it models slots as if they are isolated. So, Tulintseff's method doesn't guarantee to satisfy desired pattern and input match specifications at the end of the design. In literature search, no work on the design of microstrip-fed slot arrays including mutual coupling effects is found. Although the reciprocity theory based full-wave analysis method proposed by Pozar accurately analyzes the slot array, its utilization in the design procedure is not practical since the analysis method does not provide any closed-form expressions in terms of the offset and length of the slots. In that method, the MoM matrix equation needs to be solved for each different slot length and offset combinations and the design of the array requires multiple analysis of the array until the design specifications are satisfied. Therefore, the aim of this thesis is to construct an equivalent circuit model of the array that incorporates the mutual coupling effects between the array elements. To achieve this goal the studies conducted by Elliott for the analysis and design of slotted waveguide arrays are investigated. Elliott introduced the active impedance concept that includes the mutual coupling effects between the array elements in addition to the self impedance of an isolated slot antenna [12]. In [12], longitudinal slots cut on the broad wall of a waveguide is modeled by a shunt impedance model and closed form expression for this shunt impedance model in the presence of other slots in the array model is developed to analyze and design the whole array. Elliott also reports numerous studies on waveguide fed slots of different orientations including broad-wall inclined slots that are modeled by series impedance like microstrip line fed slots [13]. Besides waveguide fed slots, similar analysis and design equations for stripline fed slot arrays of different orientations are reported by him in [14] and [15]. However, similar design equations for microstrip line fed slot arrays are not found in literature. The main reason for the lack of those equations for microstrip line configuration might be the difficulties in computing the modal fields of a microstrip line. As it is well-known, closed-form expression for the TE and TM modes of a waveguide and TEM modes of a strip line are available. However, the modal fields of a microstrip line are quasi-TEM modes and they can not be expressed exactly in closed-form unless the microstrip line is a boxed configuration. In this thesis, modal fields of a microstrip line are expressed in closed-form by utilizing the Discrete Complex Images Method (DCIM) [18] and the design equations for microstrip line fed slot antenna arrays are derived.

In chapter 2, characterization procedure of transverse slots cut on the ground plane of a microstrip line are presented. The variation of the self impedance of an isolated slot with changes in its length and position are investigated.

Chapter 3 starts with a review of the design procedure of microstrip line fed slot antenna arrays using equivalent circuit model that ignores mutual coupling effects. By using this method, a traveling wave type linear microstrip-fed slot antenna array with 6 slots is designed targeting 6 GHz center frequency. The designed antenna is manufactured and measurement results are compared with electromagnetic simulation results and with design specifications. It is concluded that the mutual coupling effects need to be included in the equivalent circuit model. Then, expressions for the series impedance model that encounters for mutual coupling effects are derived. The accuracy of the proposed expressions is verified through a two slot configuration which is also analyzed by electromagnetic simulation software. Finally, the previously designed array is analyzed using the derived expressions and results are compared with simulation results. 2.5D MoM based software IE3D by Zeland, 3D Finite Integration Time Domain (FITD) method based time domain solver and Finite Element Method based frequency domain solver of CST Microwave Studio software are used for electromagnetic simulations.

CHAPTER 2

SLOT IMPEDANCE CHARACTERIZATION

2.1 Transverse Series Slot and Its Equivalent Circuit Model

Transverse series slots are formed by printing narrow rectangular slots of which longitudinal direction is orthogonal to the longitudinal direction of the microstrip line on the ground plane of the microstrip line (Figure 2.1).

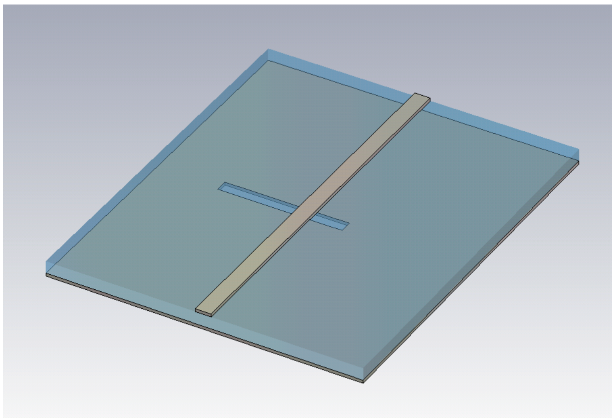

Figure 2.1: Microstrip-fed Transverse Slot

Surface current on the ground plane of a microstrip line flows along the longitudinal direction and its density decreases as moving away from the line in the transverse direction. As demonstrated by the simulation results shown in Figure 2.2, a transverse slot cut on the ground plane perturbs the longitudinal currents on the conductor and radiation occurs. **E**-field induced by surface current along the slot aperture sets the polarization of the radiation. Polarization of the radiation from slot is orthogonal to the longitudinal direction of the slot. Surface current in opposite direction inverses the polarization of the **E**-field. Magnitude of the induced **E**-field, so amount of the radiated power, reduces as offset of the slot increases. As slot moves farther away from the line, surface currents decay and no current is cut by slot. So no radiation occurs.

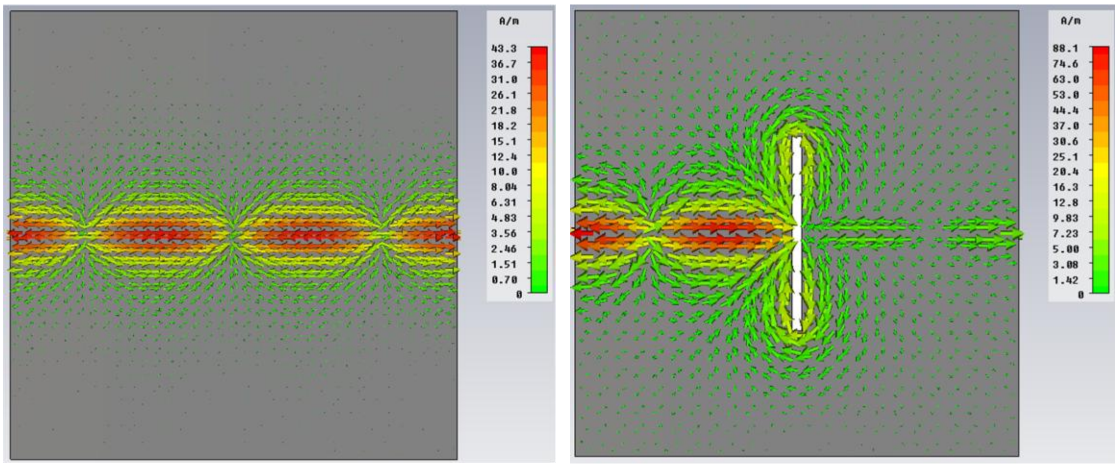

(a) **(b)**

Figure 2.2: (a) Surface currents on the ground plane of a microstrip line and (b) Surface currents on the ground plane of the same microstrip line when a transverse slot is cut.

To construct a cascaded series array of slots, an equivalent circuit model is needed. In [7], it is shown that a transverse series slot fed by a microstrip line behaves like a series impedance to the microstrip line as shown in Figure 2.3 according to the results of analysis based on reciprocity theorem.

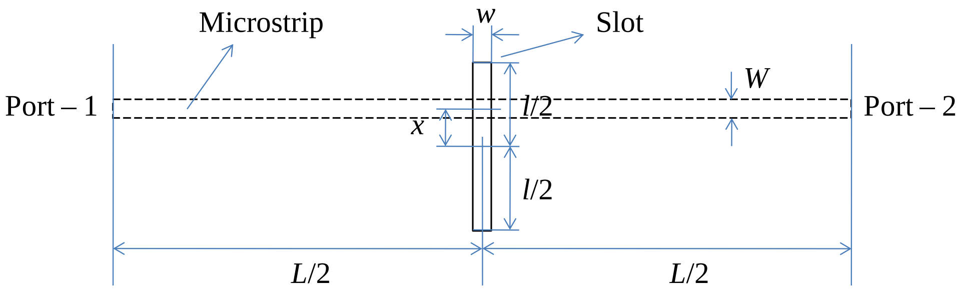

(a)

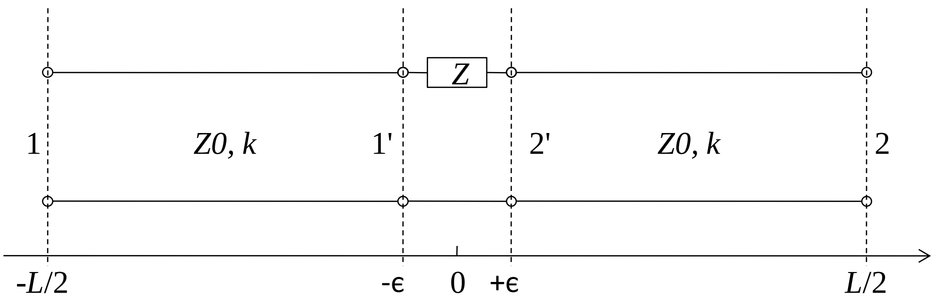

(b)

Figure 2.3: (a) Transverse Series Slot with offset, *x*, and length, *l* (b) Equivalent Circuit Model

Extraction of the series impedance value in terms of the length and offset of the slot can be done in various ways. It can be extracted experimentally by producing single microstrip-fed slots with different dimensions and measuring their S-parameters using network analyzer. Another method is extracting it numerically by analyzing the structure using commercially available electromagnetic (EM) simulation softwares. The later method is preferred in this thesis since the automatic parametric sweep tools of EM simulation softwares make the analysis fast and efficient. Also experimental method is not preferred because it requires production of many slots with reasonable mechanical tolerances and requires preparation of an experimental setup to make consistent measurements (Preparation of fixtures, identical connections etc. are needed). Hence this costly method was not chosen.

A single slot fed by a 50Ω line is analyzed using two different full-wave EM simulation tools. One is IE3D which is a MoM based 2.5D solver and the other one is the frequency domain solver of CST-Microwave Studio that is an FEM based 3D solver. Substrate of the simulated structure has dielectric constant $\varepsilon_r = 3.38$ (RO4003c) and thickness $h = 0.813$ mm. Line width (W) is 2 mm and length (L) is 60.55 mm which is two times the guided wavelength (λ_g). Slot having 1 mm width (w) and 19.845 mm length (l) is located at zero offset. Series impedance values (Detailed description of series impedance extraction is given in Section 2.2) obtained from EM simulation and measurement are presented in Figure 2.4. Simulations with CST and IE3D and measurement results show similarity. Ripples in the measurement results are considered to be caused by the effects, like SMA connectors, that are not modeled in the simulations. When the results are investigated it is seen that the slot is resonant at 6 GHz. In the following section, impedance characteristics of this slot is investigated for different positions and lengths at 6 GHz as an example to slot impedance characterization procedure that will be used in the array design.

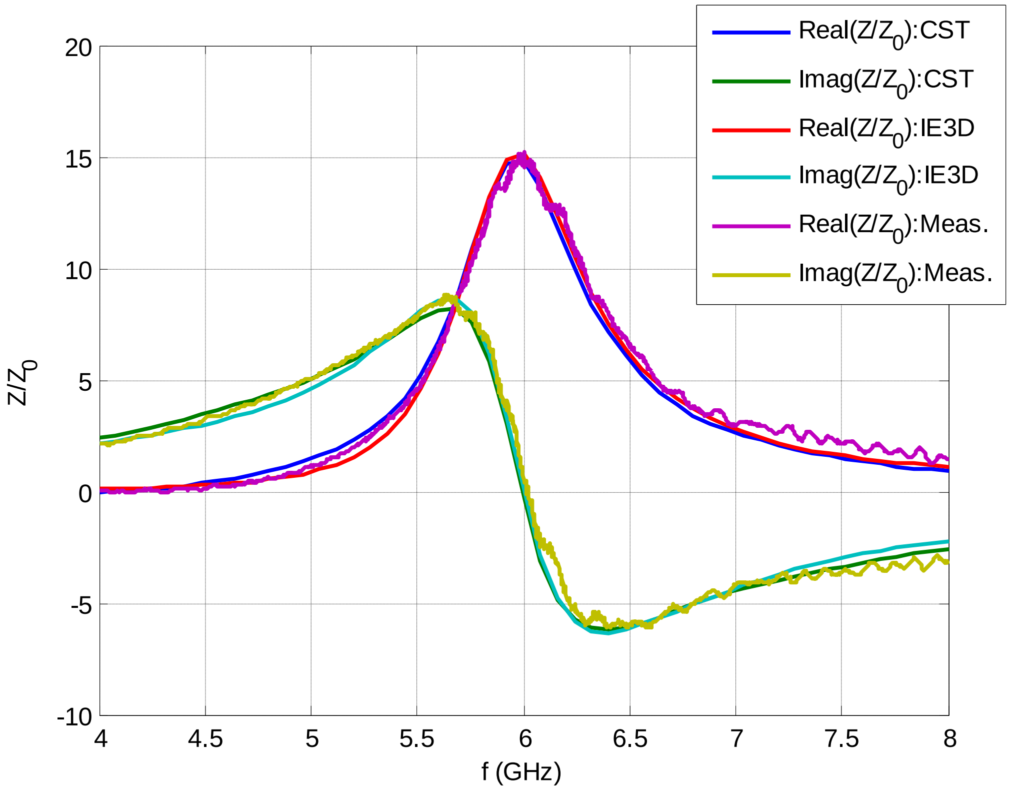

Figure 2.4: Equivalent Series Impedance of Single Slot (x = 0 mm, l = 19.845 mm, w = 1 mm) vs. Frequency for RO4003c Subs. (ϵ_r = 3.38, h = 0.813 mm), Z_0 = 50 Ω (W = 2 mm, L = 60.55 mm)

2.2 Slot Impedance Characterization Procedure

To construct an array of transverse series slots, impedance characteristics of a single isolated slot is needed in terms of dimensions and the position of the slot. Before beginning the design of the array, a fixed slot width, w, and characteristic impedance (so line width W), must be chosen (Figure 2.3.a). Then for the variables slot offset, x, and slot length, l, series slot impedance, Z, is extracted to form the curves listed below:

- Resonant length, l_{res}, vs. slot offset, x.
- Resonance resistance, R_{res}, vs. slot offset, x.
- $Real(Z)/ R_{res}$ vs. l/l_{res} for each x.
- $Imag(Z)/ R_{res}$ vs. l/l_{res} for each x.

As mentioned in the previous section series impedance, Z, can be extracted in various ways and in this thesis it is extracted by using EM simulation softwares. However, in all methods, two port S-parameters of the structure in Figure 2.3.a are needed to obtain Z. To construct the impedance characterization curves listed above a procedure like in [17] is followed. In [17], impedance characterization is done experimentally for edge slots in rectangular waveguides but it is applicable to our case and experiment can be replaced by EM simulation. Steps of the impedance characterization procedure are listed below (Analyzed geometry and its equivalent circuit is seen in Figure 2.3):

i. An appropriate length for microstrip line, L, is chosen. It is a good choice to keep it long enough to reduce the effects of the evanescent modes due to scattering from the slot.

ii. First, microstrip line is simulated with no slot. Two port S-parameters (S_{11}, S_{21}, S_{12}, S_{22}) are found. Due to the symmetry of the structure S-parameter matrix is expected to be symmetric. But numerical errors in the EM simulations may cause S_{21} and S_{12} to be different. So the arithmetic mean of S_{21} and S_{12} is noted as $S_{21,ref}$ to be used in de-embedding S-parameters (carrying S-parameters reference planes to $z=0$ plane) in later steps.

$$S_{21,ref} = \frac{S_{21}+S_{12}}{2} \tag{2.1}$$

iii. Then, structure with slot having offset x, and length l is simulated and S-parameters found are de-embedded using $S_{21,ref}$. De-embedded S-parameters are indicated by primed notation as seen in (2.2) below:

$$
\begin{aligned}
S_{11}^{'} &= S_{11} / S_{21,ref} \\
S_{21}^{'} &= S_{21} / S_{21,ref} \\
S_{12}^{'} &= S_{12} / S_{21,ref} \\
S_{22}^{'} &= S_{22} / S_{21,ref}
\end{aligned} \tag{2.2}
$$

iv. Due to the symmetry of the structure again, it is expected that $S_{11}^{'} = S_{22}^{'}$ and $S_{21}^{'} = S_{12}^{'}$ should hold. However, as in step (ii), due to numerical errors in simulation these equalities may not hold. It is a reasonable approach to use arithmetic mean of S-parameters again. Resulting S-parameters are denoted by double primed notation:

$$
\begin{aligned}
S_{11}^{"} = S_{22}^{"} &= \frac{S_{11}^{'} + S_{22}^{'}}{2} \\
S_{21}^{"} = S_{12}^{"} &= \frac{S_{21}^{'} + S_{12}^{'}}{2}
\end{aligned} \tag{2.3}
$$

v. Now two-port de-embedded S-parameters are known. Since de-embedding has carried reference planes from $z = -L/2$ and $z = +L/2$ to $z = 0$, these S-parameters belong to the lumped series impedance Z and it can be calculated in two ways: One is using reflection parameters ($S_{11}^{"}$) and it is denoted by Z_r; the other way is using transmission parameters ($S_{21}^{"}$) and it is denoted by Z_t as stated in (2.4) below.

$$
\begin{aligned}
Z_r &= \frac{2S_{11}^{"}}{1 - S_{11}^{"}} \\
Z_t &= \frac{2(1 - S_{21}^{"})}{S_{21}^{"}}
\end{aligned} \tag{2.4}
$$

Due to the deviations from series impedance model and numerical errors in simulation Z_r and Z_t are usually found to be not equal to each other. At this point, Z is assumed to be the arithmetic mean of Z_t and Z_r.

$$Z = \frac{Z_r + Z_t}{2} \tag{2.5}$$

vi. At step (v) series impedance value Z for a slot having offset x, and length l is found. If the imaginary part of Z is not equal to zero, steps from (iii) to (v) are repeated for different slot lengths at the same offset value and the length value which makes the imaginary part zero is noted as the resonant length, l_{res}, and the real part of Z is noted as the resonance resistance, R_{res}.

vii. Steps (ii) to (vi) are repeated for different offsets to create l_{res} vs. x and R_{res} vs. x curves.

viii. For each slot offset value, Z is calculated for length values in [0.95l_{res}, 1.05l_{res}] range. Then two more curves are formed for each x: One is R/R_{res} vs. l/l_{res} and the other is X/R_{res} vs. l/l_{res} curve where $Z = R + jX$.

Slot characterization for 1 mm slot width and 2 mm line width (50 Ohms) on substrate RO4003c ($\varepsilon_r = 3.38, \tan\delta = 0.0027$) having thickness 0.813 mm is done using IE3D. Line length, L, is chosen 2 times the guided wave-length (λ_g) which is $2 \times 30.275 = 60.55$mm. In Figure 2.5, resonance lengths l_{res} at various slot offsets are plotted. Resonance resistances R_{res} at these offsets are plotted in Figure 2.6.

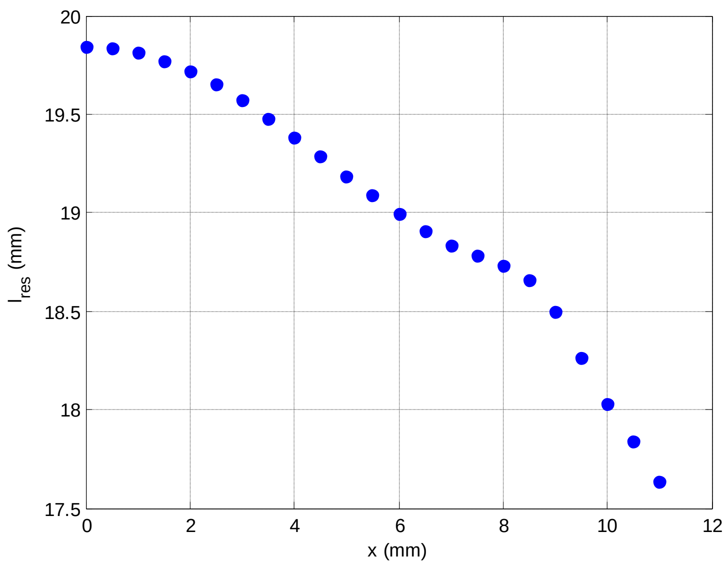

Figure 2.5: Resonance length, l_{res}, vs. slot offset, x

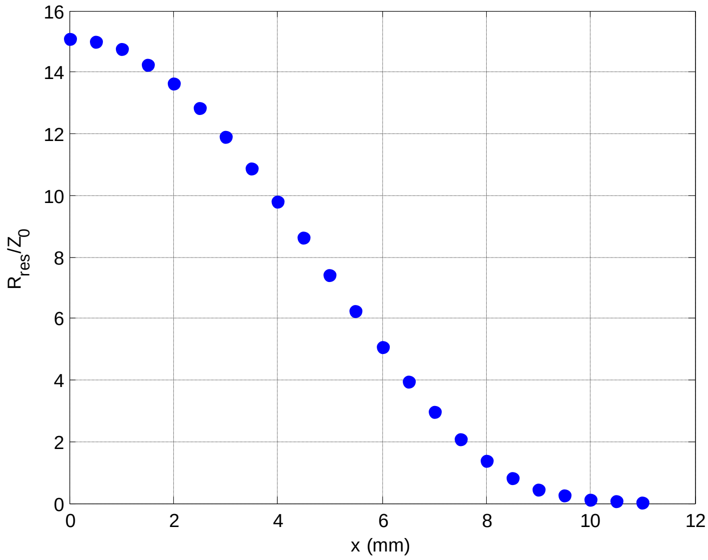

Figure 2.6: Normalized resonance resistance, R_{res}/Z_0, vs. slot offset, x, Z_0 = 50 Ω

In Figure 2.7, behavior of the real and imaginary parts of the slot impedance Z with length is shown. At each offset, Z is calculated around the resonance length in the range between $0.95\times l_{res}$ and $1.05\times l_{res}$ and normalized with R_{res} for the related offset.

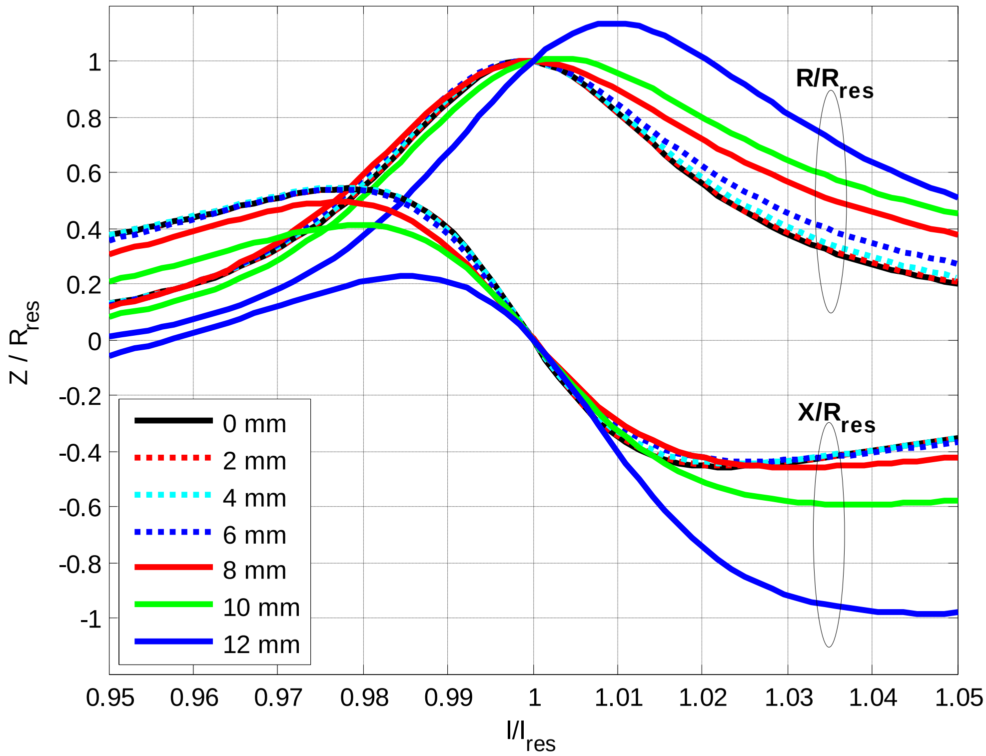

Figure 2.7: Normalized slot impedance, $Z/R_{res}=R/R_{res}+jX/R_{res}$, vs. normalized l/l_{res} for different offset values

As seen in the graph, curves for different offsets exhibit similar behavior, deviations from the general trend starts to occur for large offset values. It should be noted that the length of the slot is about 18mm, so after an offset value of 9mm, the slot has no overlapping region with the microstrip line. Hence the results for offset values larger than about 8mm's are not meaningful in practice. However, the simulation results for those offset values are also included in the figures to demonstrate the validity region of the slot characterization procedure.

The similarity in the simulation results, as shown in Figure 2.7, leads a general expression for Z that can be used for all offset values up to half of the slot length:

$$Z(x,l) = R_{res} \; s_1(x, l/l_r) + j s_2(x, l/l_r) \tag{2.6}$$

In (2.6), R_{res} and l_{res} are resonant resistance and resonant length, respectively, at offset x and they can be expressed as a function of x by fitting polynomials to the curves in Figure 2.5 and Figure 2.6, respectively. s_1 is a function of x and normalized length l/l_r and it can be formed by polynomial fitting to arithmetic mean of R/R_{res} curves for different offsets where the curves exhibit similar behavior in Figure 2.7. And, s_2 is found by fitting polynomial to arithmetic mean of X/R_{res} curves. By this way, equivalent series impedance Z can be expressed as a function of offset x and length l using 4 functions, R_{res}(x), l_{res}(x), s_1(x,y) and s_2(x,y) for $y = l / l_{res}(x)$, in the region where the curves in Figure 2.7 exhibits similar behavior around $y = 1$. These functions provide a single expression for the calculation of the self impedance of an isolated slot that will be utilized later in the design of the array.

CHAPTER 3

DESIGN OF LINEAR ARRAYS

3.1 Design Ignoring Mutual Coupling Effects

As mentioned earlier, single transverse slot can be modeled as series impedance to transmission line. Linear array of slots are formed by placing slots on the ground plane by distinct intervals as in Figure 3.1.a.

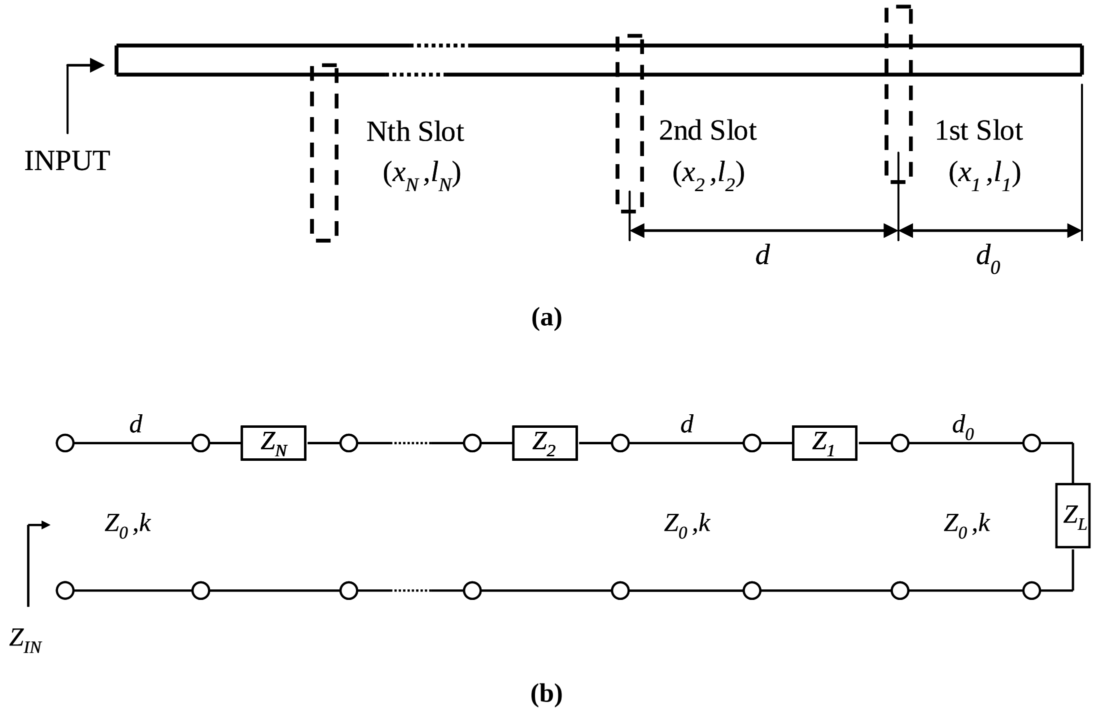

Figure 3.1: (a) Linear Series Slot Array (b) Equivalent circuit model

In [11], linear arrays are modeled by the equivalent circuit shown in Figure 3.1.b. In this equivalent circuit each slot is modeled by a series impedance. This series impedance is the same as the impedance of the single isolated slot (self-impedance) with offset x_n and length l_n which is extracted for different slot offset and lengths in

Section 2.2. Slots are modeled by their self-impedance although they are in array environment and this means the mutual coupling between the slots are ignored. Microstrip lines between the slots are modeled by transmission lines having the same characteristic impedance Z_0 and wave number $k = \beta - j\alpha$ (β : propagation constant, α : attenuation constant) with microstrip line. Equivalent transmission lines have length d which is inter-slot spacing. Design using this equivalent circuit model starts by specifying array excitation coefficients, desired input impedance and termination. Then, impedance values in the equivalent circuit model are found from desired specifications using recursive expressions relating the radiated power from slots and equivalent impedances. Lastly, slot offsets and lengths are set to values that give desired impedance values by using slot characterization data.

In the derivation of recursive expressions for the synthesis of the array, the first equation used is the equality of the radiated power from each slot to the power dissipated on its equivalent series impedance. Power radiated from n^{th} slot is expressed as

$$P_n = \frac{|I_n|^2 R_n}{2} \tag{3.1}$$

where n^{th} equivalent series impedance is $Z_n = R_n + jX_n$. I_n is the current flowing on n^{th} series impedance as seen in Figure 3.2. Phase of I_n sets the phase of the excitation coefficient of the slot and dissipated power sets the amplitude of the excitation coefficient.

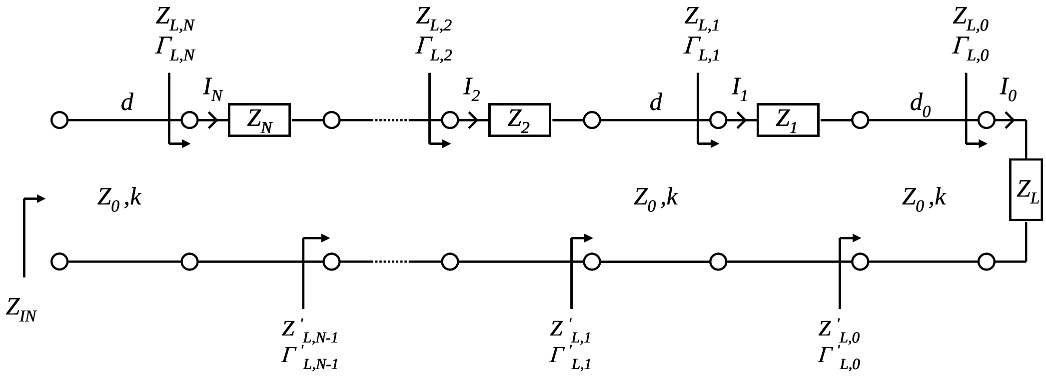

Figure 3.2: Linear Series Slot Array Equivalent Circuit Model

Second equation is derived by considering the equivalent circuit in Figure 3.2 in terms of unit cells shown in Figure 3.3.

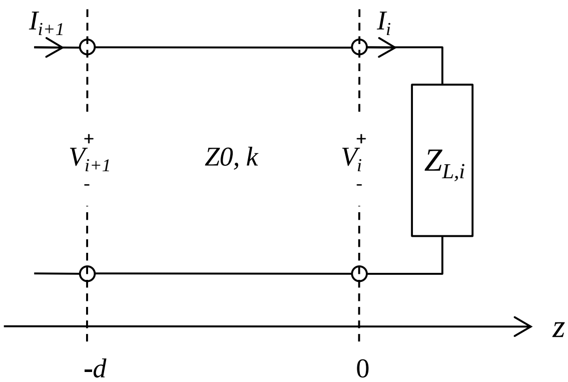

Figure 3.3: Series Slot Array Unit Cell

For each unit cell, voltage and current on the transmission line as a function of z is given by the equations:

$$\begin{aligned} V(z) &= V_i^+ e^{-jkz}\left[1+\Gamma_{L,i} e^{j2kz}\right] \\ I(z) &= \frac{V_i^+}{Z_0} e^{-jkz}\left[1-\Gamma_{L,i} e^{j2kz}\right] \end{aligned} \tag{3.2}$$

where $i = 0,1,\ldots,N$. Ratio of currents at $z = 0$ and $z = -d$ planes, gives the equation below:

$$\frac{I(z=-d)}{I(z=0)} = \frac{I_{i+1}}{I_i} = \frac{1-\Gamma_{L,i}e^{-j2kd}}{1-\Gamma_{L,i}} e^{jkd} \tag{3.3}$$

Rearranging (3.1) and substituting (3.3) in it give

$$R_i = \frac{2P_i}{\left|I_i\right|^2} = \frac{2P_i}{\left|I_{i-1}\right|^2} \frac{\left|1-\Gamma_{L,i-1}\right|^2}{\left|1-\Gamma_{L,i-1}e^{-j2kd}\right|^2} \tag{3.4}$$

where

$$\begin{aligned} \Gamma_{L,i} &= \frac{Z_{L,i}-Z_0}{Z_{L,i}+Z_0} \\ Z_{L,i} &= Z_i + Z'_{L,i-1} \\ Z'_{L,i} &= \frac{Z_{L,i} + jZ_0 \tan kd}{Z_0 + jZ_{L,i} \tan kd} \end{aligned} \tag{3.5}$$

Using the expressions derived above an iterative design procedure is followed to synthesize arrays without considering mutual coupling effects. In [11], series impedances are always assumed to be pure real so slot lengths are chosen to be the resonant length. Steps of the design procedure for an array of N slots are as follows:

i. Array excitation coefficients of the desired far-field pattern are determined $(a_1, a_2, \ldots, a_N)$. Phase progress between array elements are kept same for simplicity but the procedure can be extended to non-uniform phase case. Uniform phase progress between array elements, ψ, determines the inter-element spacing *d* by the relationship:

$$\psi = -\beta d \tag{3.6}$$

Relationship between ψ and the main beam offset from the broadside angle θ_0 is

$$\psi = -\beta d = \pm k_0 d \sin\theta_0 + 2\pi m \tag{3.7}$$

where $m = 0, \pm 1, \pm 2, \ldots$.

ii. Termination of the array Z_L is specified. For broadside arrays (resonant arrays) ($\theta_0 = 0$) all slot impedances should be resonant and it is good choice to set the impedance seen after first slot ($Z_{L,0}^{'}$) as pure real and low to provide good impedance match at the input since all slot resistances are added to each other. General way is to set $Z_{L,0}^{'}$ to zero by making $Z_L = \infty$ (open-circuit) and transforming by quarter-wave transformer or by making $Z_L = 0$ (short-circuit) and carrying it by half wavelength line. For offset beam arrays (traveling-wave arrays) ($\theta_0 \neq 0$), Z_L should be set to Z_0 to prevent reflections that will result in undesired second beam.

iii. Radiated power from each slot is proportional to the square of the amplitude of the excitation coefficients ($P_n \,\alpha\, |a_n|^2$). It is assumed that $P_n = |a_n|^2$ for $n = 1, 2, \ldots, N$.

iv. An initial guest for the first slot impedance $Z_1 = Z_1^{'}$ (It should be pure real since slots are assumed to be resonant) is made. This step is the starting point of iterations.

v. I_1 is calculated from (3.1) and $\Gamma_{L,1}$ is calculated from (3.5) to find Z_2. Real part of Z_2 is calculated from (3.4) which is

$$R_2 = \frac{2P_2}{|I_1|^2} \frac{|1-\Gamma_{L,1}|^2}{|1-\Gamma_{L,1}e^{-j2kd}|^2} \tag{3.8}$$

In [11], it is said that phase shift between slots is determined by phase of *I* flowing on each node. This means $\angle I_2 = \angle I_1 + \beta d$ should be satisfied and this requires that imaginary part of the first term in right hand side of (3.3) must be equal to zero as stated below.

$$\mathrm{Im}\left\{ \frac{1-\Gamma_{L,1}e^{-j2kd}}{1-\Gamma_{L,1}} \right\} = 0 \tag{3.9}$$

However, (3.9) is not satisfied for some *d* values when series impedances are chosen pure real. There occurs a slight difference in phase of current at nodes from desired phase shift. This breaks the assumption that connects phase shift and phase of the current. Since this doesn't cause too much difference in phase it can be omitted.

vi. Steps (iv) and (v) repeated for all remaining slots then all Z_i's for $i = 1, 2, \ldots, N$ are found. This step is the end of iterations.

vii. Z_{IN} $(= Z'_{L,N})$ and ratio of power dissipated on load (for traveling wave arrays) are checked whether they are in desired limits or not. If it is not, new iterations are done by changing the initial guess Z'_1 until the desired values are achieved.

viii. After series impedances for all slots are found, slot lengths and offsets that give these impedance values are determined using slot characterization data.

At the center frequency of at 6 GHz, a linear traveling-wave array having 6 slots is designed using this method for the parameters listed below:

- Substrate: RO4003c ($\varepsilon_r = 3.38, \tan\delta = 0.0027 @ 10\,GHz$) 32 mil (0.813 mm) thickness, ½ oz (17 um) Copper.
- Line: Width (W) = 2 mm (50 Ohms), $\lambda_g = 30.275\,\text{mm}$, $\beta = 207.54\,\text{m}^{-1}$, $\alpha = 0.349\,\text{m}^{-1}$
- Slot width (w) = 1 mm
- Inter-slot spacing: $d = 0.75\lambda_g$ ($\psi = \beta d = 270^\circ$) (Main-beam direction is at 33^o offset from broad-side)
- Array Excitation Coefficients: $|a_n|$ = [0.8 0.9 1.0 1.0 0.9 0.8] (Gives 15 dB sidelobe reduction, 24^o 3dB beam-width)
- Termination is matched load (Z_L = 50 Ohms).

Series impedance values, slot offsets and lengths found after synthesis using these parameters are seen in Table 3.1. In synthesis, S_{11} is set to -15.4 dB and ratio of power dissipated on load to power accepted by antenna is set to %11.3. This antenna synthesized using method ignoring mutual coupling effects was simulated using FITD (Finite Integration Time Domain) method based time domain solver of CST Microwave Studio. Also the antenna was manufactured and measured to compare with the simulation results (Figure 3.4).

Table 3.1: Slot Offsets and Lengths of Linear Traveling-Wave MS-fed Slot Antenna Array

Slot No.	$\|a_n\|$	Z/Z_0	x (mm)	l (mm)
1	0.8	1.000	8.316	18.689
2	0.9	0.314	9.319	18.352
3	1.0	0.566	8.834	18.560
4	1.0	0.177	9.768	18.134
5	0.9	0.254	9.487	18.269
6	0.8	0.078	10.440	17.860

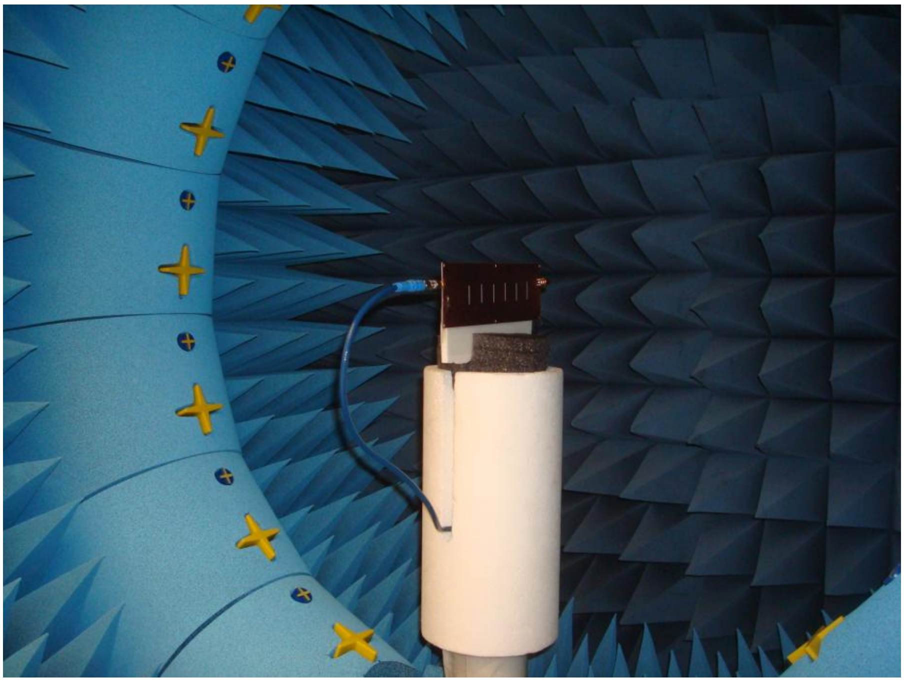

Figure 3.4: Linear Traveling-Wave MS-fed Slot Array Antenna in Spherical Near Field Test Range

S-parameters of the antenna are shown in Figure 3.5. Agreement between simulation results and measurement is observed. S-parameters are for two ports because second port of the network analyzer is connected instead of load to measure power dissipated on load. During the synthesis of the array S_{11} is set to -15.4 dB but measured value is -12.5 dB. According to synthesis S_{21} should be -9.7 dB and it is measured as -10 dB. Measured antenna radiation efficiency is %89 (Input mismatch is not included) while it is calculated as %88.7 after synthesis.

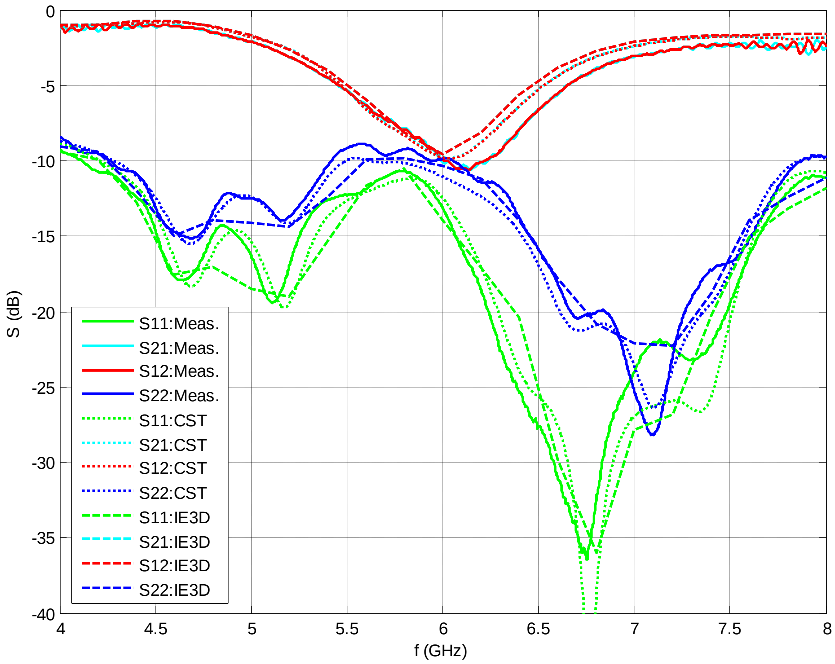

Figure 3.5: S-parameters of Linear Traveling-Wave MS-fed Slot Array Antenna

Measured and simulated azimuth radiation patterns of the antenna and desired array factor is shown in Figure 3.6. Referring to the figure, azimuth plane is the one in which $\theta = 90^\circ$ and ϕ changes between 0^o and 360^o. Co-polarization component of the field corresponds to θ component, and cross-polarization component corresponds to ϕ component of the **E**-field. As seen in the figure, agreement between CST and measurement results in main beam and side-lobe levels is observed. There is an approximately 4^o shift in main beam direction when compared with desired pattern and sidelobes are nearly 3.5 dB higher than the desired value. This type of antenna also radiates to back half-space. Since the effects of mutual coupling and design including mutual coupling is investigated in this work, no attention to radiation in backward direction is taken. Backward radiation can be prevented by placing a ground plane at a certain distance and parallel to the antenna as reported in [5].

Two more antennas are designed to see the effects of the choice of the first slot impedance on antenna efficiency and to observe synthesis results for a desired radiation pattern with lower sidelobe levels.

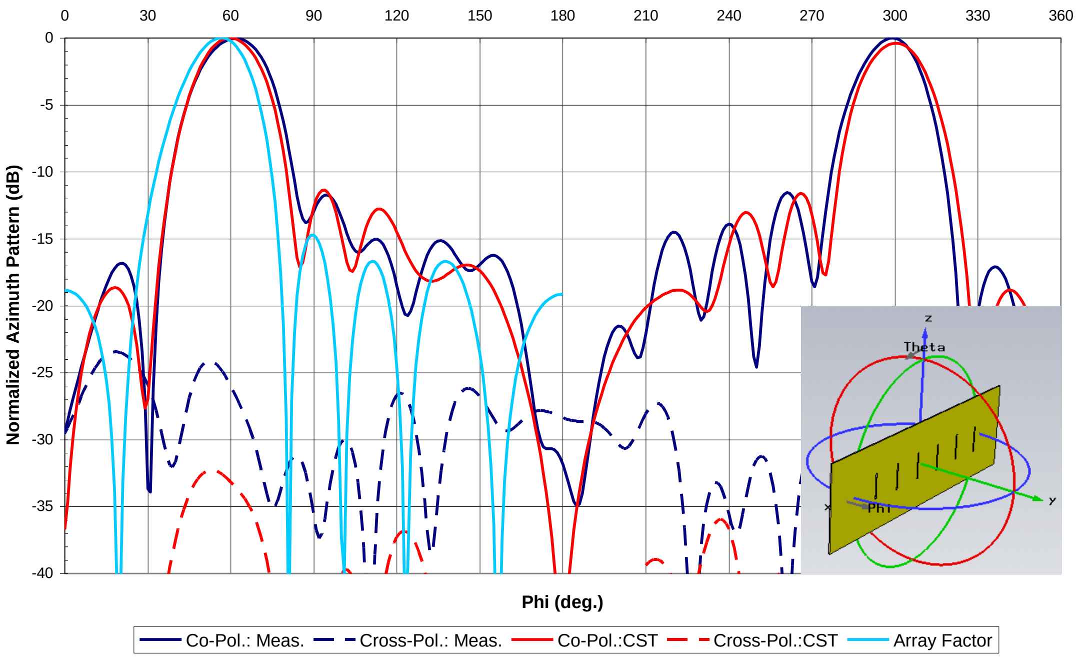

Figure 3.6: Normalized Azimuth Pattern of Linear Traveling-Wave MS-fed Slot Array Antenna

Second antenna is synthesized for same design specifications listed in the previous example. In this design, Z_1 / Z_0 is set to 3 to lower the amount of power dissipated at matched load termination. Although making $Z_1 / Z_0 = 3$ causes input mismatch (According to synthesis result S_{11} becomes -7.9 dB), ratio of power dissipated on load to accepted power decreases, so antenna radiation efficiency increases. Equivalent impedance values, slot offsets and lengths for this antenna are listed in Table 3.2. Antenna input impedance is matched by a quarter-wave transformer at 6 GHz (Since results of synthesis at 6 GHz is investigated, broadband matching was not aimed). S-parameters of the antenna are shown in Figure 3.7 and the azimuth pattern is shown in Figure 3.8. Radiation efficiency of the antenna is calculated as %96.2. Efficiency has increased as expected. When the pattern of the antenna is examined, disagreement between the simulated pattern and the desired pattern exists as in the measured antenna. Analyzing this antenna also shows that, although both antennas in Table 3.1 and Table 3.2 are synthesized for the same pattern, obtained patterns are not same because mutual coupling between slots in two arrays are different since slot dimensions and positions are different.

Table 3.2: Slot Offsets and Lengths of Linear Traveling-Wave MS-Fed Slot Array Antenna synthesized with Z_1/Z_0=3

Slot No.	$\lvert a_n \rvert$	Z/Z_0	x (mm)	l (mm)
1	0.8	3.000	6.984	18.840
2	0.9	0.236	9.542	18.242
3	1.0	1.159	8.172	18.711
4	1.0	0.116	10.130	17.976
5	0.9	0.468	8.995	18.502
6	0.8	0.050	10.864	17.698

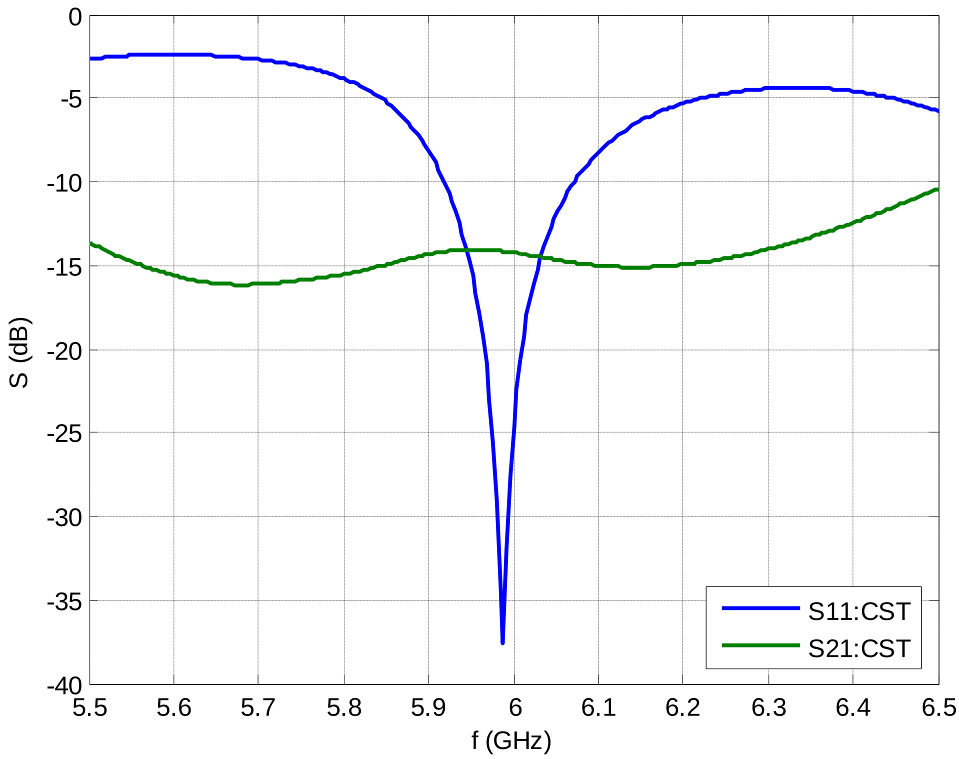

Figure 3.7: S-parameters of Linear Traveling-Wave MS-fed Slot Array Antenna synthesized with Z_1/Z_0=3

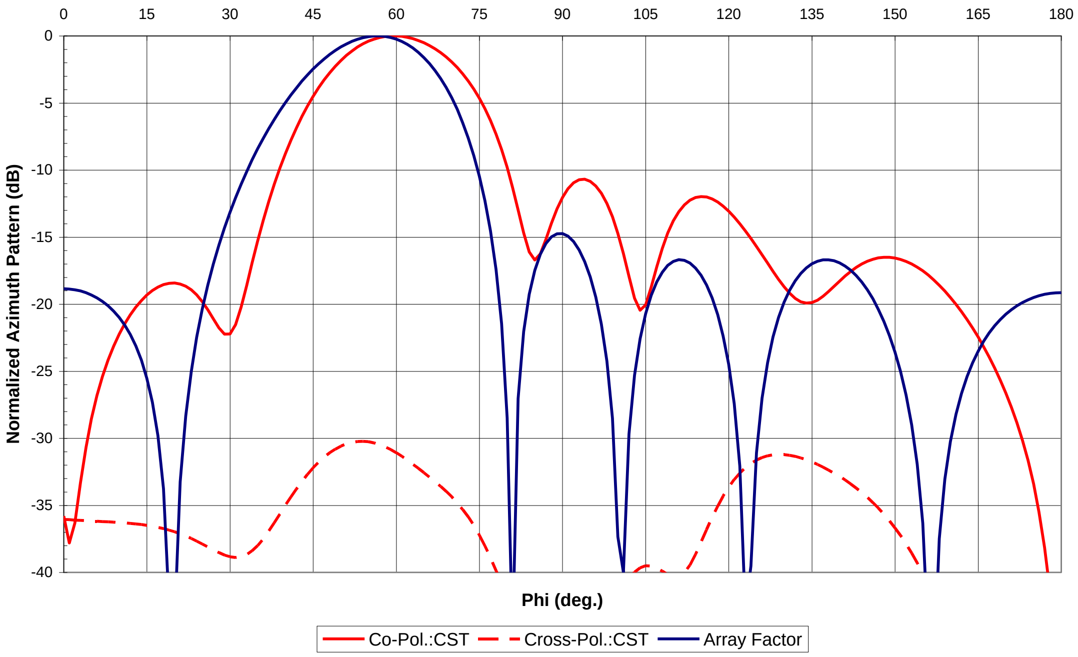

Figure 3.8: Normalized Azimuth Pattern of Linear Traveling-Wave MS-fed Slot Array Antenna synthesized with Z_1/Z_0=3

Another antenna with 6 slots is synthesized for 20 dB sidelobe level and for same main lobe direction with previously analyzed antennas. Excitation coefficients, slot offsets and lengths are seen in Table 3.3. Antenna is synthesized by setting $Z_1 / Z_0 = 3$ again. In Figure 3.9, S-parameters of the antenna are shown. Input impedance is matched at 6 GHz using a quarter-wave transformer again. Radiation efficiency of the antenna is %98.3. In Figure 3.10, azimuth pattern of the antenna is presented. It is seen that shift in main-lobe direction occurs for synthesis done by 20 dB sidelobe level distribution. Also, sidelobe level is 5 dB higher than target value.

Table 3.3: Slot Offsets and Lengths of Linear Traveling-Wave MS-Fed Slot Array Antenna synthesized for 20 dB sidelobe level

Slot No.	$\lvert a_n \rvert$	Z/Z_0	x (mm)	l (mm)
1	0.55	3.000	6.984	18.689
2	0.78	0.376	9.176	18.352
3	1.00	1.503	7.898	18.560
4	1.00	0.159	9.850	18.134
5	0.78	0.387	9.152	18.269
6	0.55	0.033	11.150	17.860

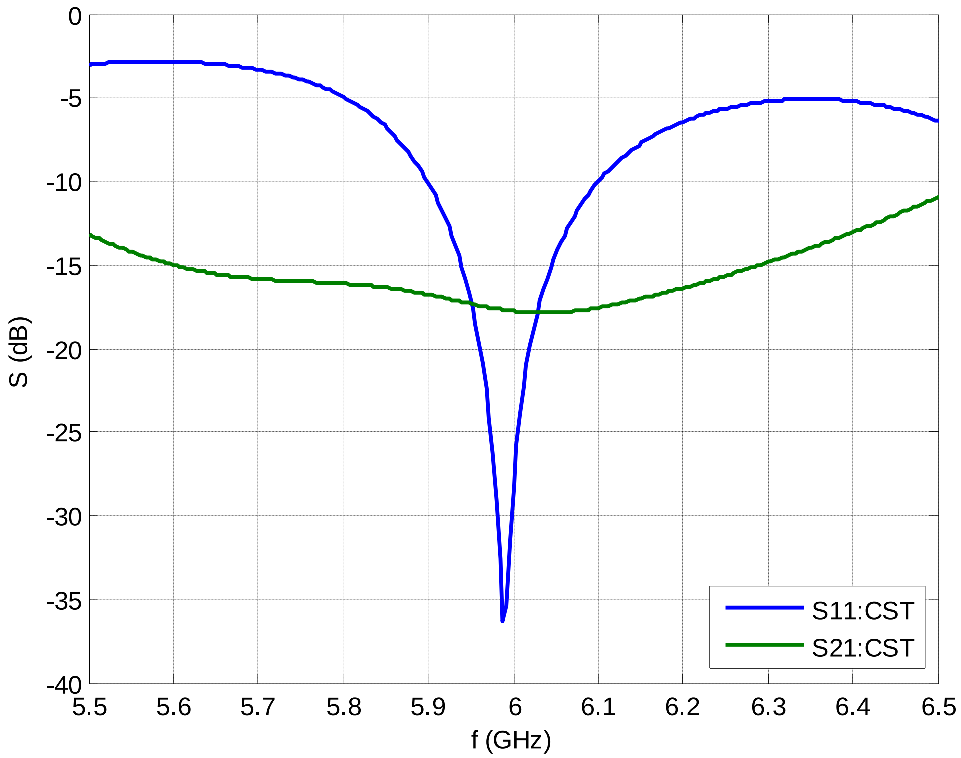

Figure 3.9: S-parameters of Linear Traveling-Wave MS-fed Slot Array Antenna synthesized for 20 dB sidelobe level

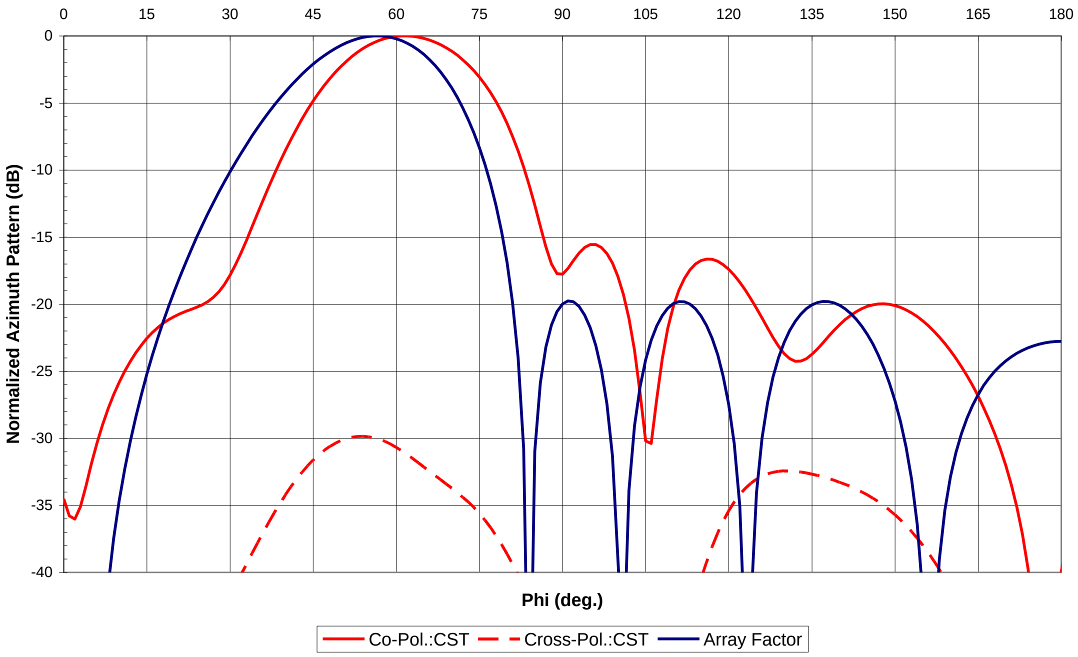

Figure 3.10: Normalized Azimuth Pattern of Linear Traveling-Wave MS-fed Slot Array Antenna synthesized for 20 dB sidelobe level

As seen in results, array synthesized by described method in this section does not provide the desired performance. In literature, no design method including mutual coupling effects for microstrip line fed slot arrays is found. In the next section, works done for the development of an analysis and design method that incorporates mutual coupling effects into the equivalent circuit model are presented.

3.2 Analysis Including Mutual Coupling Effects

Pozar makes a full-wave analysis for a microstrip-fed slot by using reciprocity method in [7] as it is done for waveguide-fed slots and boxed stripline-fed slots by Elliott in [12] and [15], respectively. In this work, expressions for the reflected and transmitted waves on the microstrip-line are derived using Green's functions for the grounded dielectric slab. The analyzed geometry is seen in Figure 3.11.

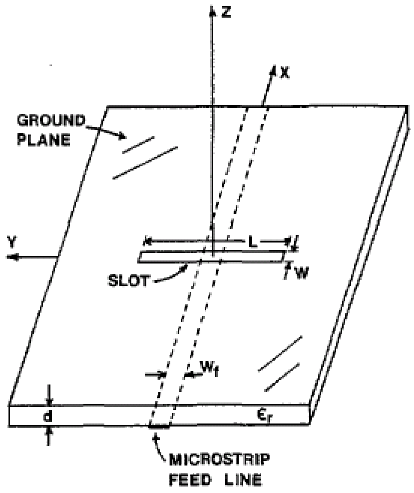

(a)

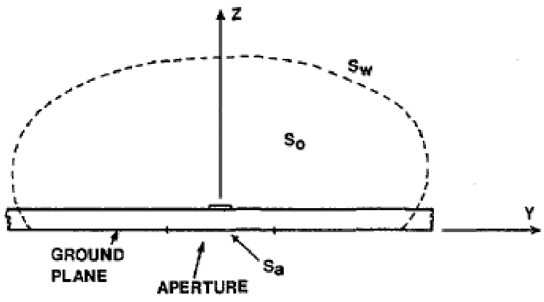

(b)

Figure 3.11: (a) Slot fed by infinite microstrip-line and (b) Surfaces defined for reciprocity analysis [7]

In analysis, the microstrip line is infinitely long and quasi-TEM mode propagates with modal fields

$$\bar{e}(y,z) = e_y\hat{y} + e_z\hat{z},$$
$$\bar{h}(y,z) = h_y\hat{y} + h_z\hat{z}. \tag{3.10}$$

Fields in (3.10) are normalized expressions that satisfy

$$\int_{y=-\infty}^{\infty}\int_{z=0}^{\infty} \bar{e}\times\bar{h}\cdot\hat{x}\, dy\, dz = 1. \tag{3.11}$$

Forward and backward traveling microstrip line fields are defined as

$$\bar{E}^{\pm} = \bar{e}e^{\pm j\beta x},$$
$$\bar{H}^{\pm} = \pm\bar{h}e^{\pm j\beta x}, \tag{3.12}$$

where β is the propagation constant of the line (Up to this point, x is used for slot offset with respect to line center in $\pm y$ direction in Figure 3.11. In the remaining part, x will represent space coordinate and x_{off} will be used for slot offset). β and the modal fields are found using spectral domain Green's functions given in [7].

However, β is found by EM simulation where it is need in this thesis. Total microstrip line fields are written as below while slot discontinuity center is located at $x = 0$.

$$\bar{E} = \begin{cases} \bar{E}^{+} + R\bar{E}^{-} & for\ x < 0 \\ T\bar{E}^{-} & for\ x > 0 \end{cases}$$
$$\bar{H} = \begin{cases} \bar{H}^{+} + R\bar{H}^{-} & for\ x < 0 \\ T\bar{H}^{-} & for\ x > 0 \end{cases} \tag{3.13}$$

R and *T* are the reflection and transmission coefficients, respectively. Applying the reciprocity theorem for total microstrip line fields and positive traveling components gives the expression below:

$$\int_S \bar{E} \times \bar{H}^{+} \cdot d\bar{s} = \int_S \bar{E}^{+} \times \bar{H} \cdot d\bar{s} \tag{3.14}$$

Integrals are over the surface $S = S_0 + S_a + S_w$ where

- S_0 is the cross section of the microstrip line ($-\infty < y < \infty$ and $0 \le z < \infty$),
- S_a is the slot aperture surface,
- S_w is area occupied by the walls of the microstrip line ($y \to \pm\infty$, $z \to \infty$ and $z = 0$).

Integrals evaluated over S_0 contributes zero. On S_a, $\hat{n} \times \bar{E}^{+} = 0$ and $\hat{n} \times \bar{E} = V_0 \hat{n} \times \hat{x} e_x^a$ where $\hat{x} V_0 e_x^a$ is the unknown aperture field. Aperture filed is approximated by piecewise sinusoidal functions in the method of moments analysis done in [7]. However, for analysis of array antennas in this section, it will be approximated by a single function given below as it is done in reciprocity analysis for strip line fed slots in [14].

$$V_0 e_x^a = \frac{V_0}{w} \cos\frac{\pi y}{l} \quad for \quad |x| < w/2, |y| < l/2 \tag{3.15}$$

To return the evaluation of reciprocity expression, integrals over S_a and S_0 yields the equation

$$R = \frac{V_0}{2}\Delta v \tag{3.16}$$

where

$$\Delta v = \int_{S_a} e_x^a(x, y - x_{off}) h_y(x, y) ds. \tag{3.17}$$

Reciprocity theorem can also be written for total microstrip line fields and field components for waves traveling in negative direction as

$$\int_S \bar{E} \times \bar{H}^- \cdot d\bar{s} = \int_S \bar{E}^- \times \bar{H} \cdot d\bar{s}, \tag{3.18}$$

Then the transmission coefficient can be found as

$$T = 1 - \frac{V_0}{2}\int_{S_a} e_x^a(x, y - x_{off}) h_y(x, y) ds = 1 - R. \tag{3.19}$$

$T = 1 - R$ equality shows that the slot can be modeled as a series impedance to transmission line. This is the analytical evidence of series impedance model.

Up to this point, expressions for the unknowns R and T are found in terms of another unknown V_0. To find the third equation for the solution of these three unknowns, continuity of H_y across aperture is imposed as

$$H_y^e = H_y^f + H_y^i \tag{3.20}$$

where

- H_y^e is the exterior field ($z < 0$) due to aperture field,
- H_y^i is the interior field ($z > 0$) due to aperture field,
- H_y^f is the interior field ($z > 0$) due to line modal fields.

This condition yields the equation

$$V_0 Y^e = \Delta v(1-R) \tag{3.21}$$

where

$$Y^e = \int_{S_a}\int_{S_a} e_x^a(x,y)\, G_{yy}^{HM}(x,y;x_0,y_0)\, e_x^a(x_0,y_0)\, ds\, ds_0. \tag{3.22}$$

G_{yy}^{HM} is the Green's function that gives H_y at $(x,y,0)$ due to a $\hat{y}$ directed unit magnetic current (equivalent to e_x^a slot aperture field) at $(x_0,y_0,0)$ and spectral domain expression for it is given by equation (A.4) in Appendix-A. By this third equation V_0, R and T is written as below:

$$V_0 = \frac{2\Delta v}{\Delta v^2 + 2Y^e} \tag{3.23}$$

$$R = \frac{\Delta v^2}{\Delta v^2 + 2Y^e} \tag{3.24}$$

$$T = 1 - R = \frac{2Y^e}{\Delta v^2 + 2Y^e} \tag{3.25}$$

Then series impedance value is found as

$$Z = Z_0 \frac{2R}{1-R} = Z_0 \frac{\Delta v^2}{Y^e}. \tag{3.26}$$

In [7], equations (3.23) to (3.26) are used to calculate R, T and Z by applying the MoM procedure.

In order to find an equivalent model that incorporates the mutual coupling effects, the analysis method proposed in [14] for strip line fed slot antenna arrays is investigated in detail and it is realized that the design equations given in [14] can be written in terms of equations (3.17) and (3.22) for microstrip line fed slot antenna arrays. Therefore, first the analysis method proposed in [14] will be summarized and then the design equations derived for microstrip line fed slot antennas will be presented.

Strip line fed slots are also modeled by series impedance to transmission line like microstrip-fed slot antennas. In [14], effects of mutual coupling between other slots in the array are included to series impedance model and an analysis method is derived. Slot plane is assumed to be infinitely large in this analysis. Impedance of slots in array environment is named as active impedance and denoted by Z^a. Equivalent circuit model and notations are same as in Figure 3.2 except Z_n's are replaced by Z_n^a. Expressions derived for Z^a lead to two design equations that are used in an iterative way to design arrays of given pattern requirements and input match condition. These design equations are as below:

$$\frac{Z_n^a}{Z_0} = K_1 f_n(l_n, x_{off,n}) \frac{V_n^s}{I_n} \tag{3.27}$$

$$\frac{Z_n^a}{Z_0} = \frac{f_n^2(l_n, x_{off,n})}{\dfrac{f_n^2(l_n, x_{off,n})}{Z_n / Z_0} + K_2 \displaystyle\sum_{\substack{m=1 \\ m \neq n}}^{N} \frac{V_m^s}{V_n^s} p_{mn}} \tag{3.28}$$

V_n^s is the maximum value of aperture electric field distribution of the nth slot and named as slot voltage. It is equivalent to V_0 in (3.15). Slot voltage values are determined from the desired radiation pattern. K_1 and K_2 are constants. (3.27) is the equation that relates transmission line current I_n to active impedance Z_n^a. Z_n is the self-impedance of the nth slot that is extracted by slot characterization and expressed as (2.6) by fitting polynomials to curves. p_{mn} in (3.28) is the reaction integral between nth and mth slot that is responsible for inclusion of mutual coupling effects. It is seen that if second term in the denominator is omitted, active impedance expression for (3.28) reduce to self impedance which is the impedance of an isolated slot.

For the design problem there are *2N* unknowns which are slot offsets and lengths $(l_n, x_{off,n})$. (*N-1*) equations are obtained by writing (3.27) in ratio form as below:

$$\frac{Z_n^a / Z_0}{Z_m^a / Z_0} = \frac{f_n(l_n, x_{off,n})}{f_m(l_m, x_{off,m})} \frac{V_n^s}{V_m^s} \frac{I_m}{I_n} \tag{3.29}$$

N equations are obtained by imposing the active resonance condition that corresponds to making Z_n^a pure real as follows:

$$\mathrm{Im}\left\{ \frac{f_n^2(l_n, x_{off,n})}{Z_n / Z_0} + K_2 \sum_{\substack{m=1 \\ m\neq n}}^{N} \frac{V_m^s}{V_n^s} p_{mn} \right\} = 0. \tag{3.30}$$

The last equation comes from the specification on the input impedance of the array and it is expressed as:

$$\sum_{n=1}^{N} \frac{Z_n^a}{Z_0} = Z_{IN,desired} \tag{3.31}$$

For simplicity, in equation (3.31), the input impedance of the *N* slot array is written for resonantly spaced arrays. For traveling wave arrays, the input impedance of the array needs to be calculated using equation (3.5).

To complete the design, these *2N* nonlinear equations are solved using non-linear optimization techniques.

These design equations for strip line fed slots have the same form as the ones developed for waveguide-fed structures [12]. However, the function f_n and constants K_1 and K_2 change. This gives the idea that equations (3.27) and (3.28) can be constructed for microstrip-fed slot arrays by replacing the guiding structure with a microstrip line in the analysis done in [14] and by deriving the expressions for f_n and constants K_1 and K_2.

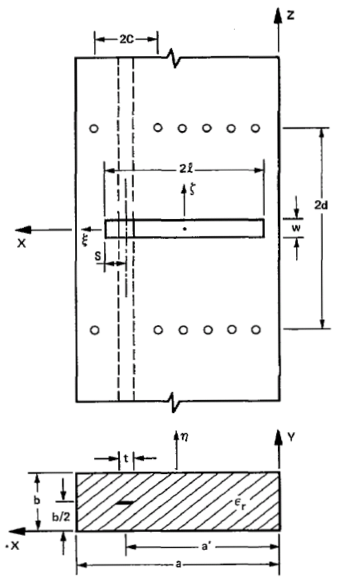

Figure 3.12: Boxed Stripline-Fed Slot [14]

In [14], f_n for the boxed strip line fed slot (Figure 3.12) is defined as

$$B_{TEM} = -C_{TEM} = V_n^s f_n(l_n, x_{off,n}). \qquad (3.32)$$

B_{TEM} and C_{TEM} are respectively the coefficients of the forward and backward scattered fields guided by the boxed strip line structure normalized with respect to the power carried by the incident field which is guided by the strip line. Since power guided by microstrip line is set to unity by imposing (3.11), B_{TEM} is equivalent to R given by (3.16) for microstrip line. Then, $R = V_n^s f_n(l_n, x_n)$ is obtained by replacing B_{TEM} with R and f_n for microstrip-fed slot becomes

$$f_n(l_n, x_{off,n}) = \frac{\Delta v}{2} = \frac{1}{2}\int_{S_a} e_x^a(x, y - x_{off,n}) h_y(x,y) ds. \qquad (3.33)$$

$h_y(x,y)$ is the y component of the magnetic field caused by the microstrip line. Closed-form expression for the spectral domain counterpart of the microstrip line guided modal field, $h_y(x,y)$, is given in Appendix A. In this expression, microstrip line current is assumed to be uniform over the width of the line. A transformation from the spectral domain to the spatial domain is required to evaluate f_n. This transformation is done by using the method offered in [16] and $h_y(x,y)$ is written in terms of complex exponentials. The variation of $h_y(x,y)$ along the length of the slot is shown in Figure 3.13 together with the assumed electric field distribution along the slot. In Figure 3.13, the offset of the slot is zero. It is evident from the figure that, when the slot offset is increased, the red curve will move towards left or right and the value of f_n, which is the reaction integral of h_y and e_x^a, will decrease.

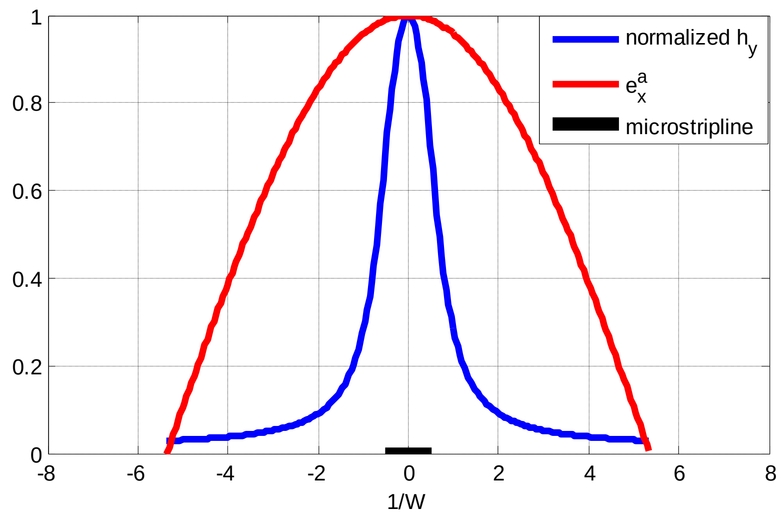

Figure 3.13: Variation of h_y and e_x^a along the length of a slot with zero offset

After f_n is found, the relation between the active impedance and mode current for microstrip line case can be written as

$$\frac{Z_n^a}{Z_0} = 2\sqrt{Z_0}\, f_n(l_n, x_{off,n}) \frac{V_n^s}{I_n} \tag{3.34}$$

where $K_1 = 2\sqrt{Z_0}$ constant is derived from power relations.

Active impedance of the n[th] slot, Z_n^a, becomes as below for the microstrip line fed slot case.

$$\frac{Z_n^a}{Z_0} = \frac{f^2(x_{off,n}, l_n)}{\dfrac{f^2(x_{off,n}, l_n)}{Z_n / Z_0} + \dfrac{jk_0}{2\eta_0} \sum_{\substack{m=1 \\ m \neq n}}^{N} \dfrac{V_m^s}{V_n^s} p_{mn}} \tag{3.35}$$

The constant $K_2 = jk_0 / 2\eta_0$ is found by power relations again. p_{mn} is the reaction integral between mth and nth slots and it is calculated for the geometry seen in Figure 3.14.

$$p_{mn} = \int_{S_{a,m}} \int_{S_{a,n}} e_x^a(x_m^{'}, y_m^{'}) G_{yy}^{HM}(x_m^{'}, y_m^{'}; x_n^{'}, y_n^{'}) e_x^a(x_n^{'}, y_n^{'}) ds_n^{'} ds_m^{'} \tag{3.36}$$

p_{mn} for strip line case in [14] is the reaction integral of two slots on the infinite perfectly conducting plane. (3.36) is obtained by changing the free-space Green's function in strip line fed slot case with the Green's function for the grounded dielectric slab, G_{yy}^{HM}, for the microstrip line fed case.

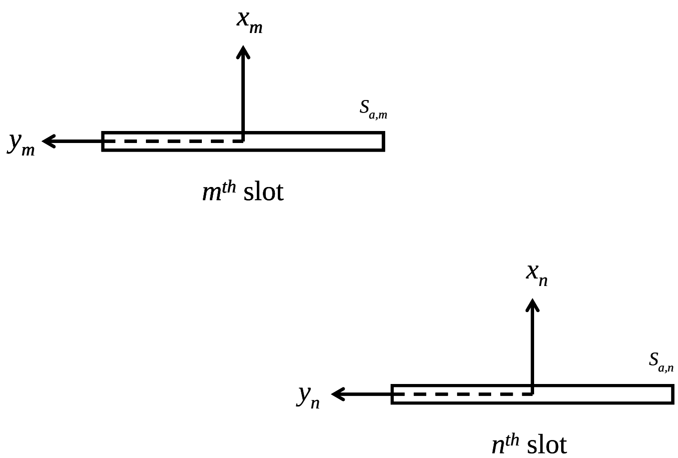

Figure 3.14: Geometry for calculation of p_{mn}

Spectral domain expression for G_{yy}^{HM} is given in Appendix A. To calculate p_{mn} the spectral domain Green's function needs to be transformed into the spatial domain. The spatial domain Green's function is also expressed in terms of complex exponentials. Then, integrals for f and p_{mn} are evaluated numerically. In order to reduce the computational cost in the evaluation of both integrals, slots are assumed to be infinitesimally thin and integrals are evaluated over one dimension (along the length of the slot) as it is done in [14].

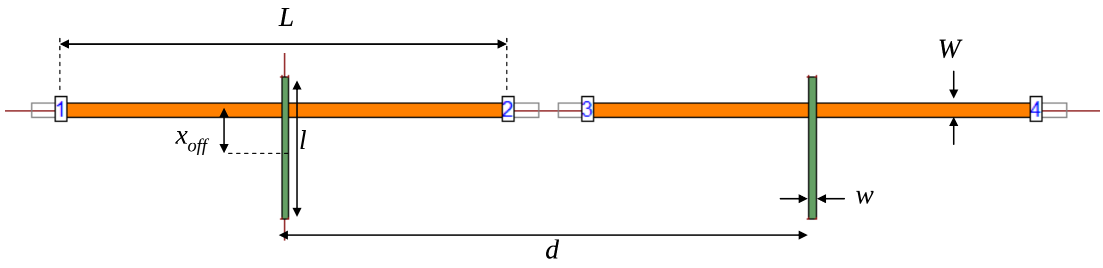

Figure 3.15: Structure consisting of two identical slots with identical feed analyzed for Z^a, RO4003c Subs. (ϵ_r = 3.38, h = 0.813 mm), W = 2 mm, L = 2xλ_g = 60.55 mm, w = 1 mm

To test the validity of expression derived for Z^a, two identical slots fed by two identical separate microstrip lines are simulated using IE3D and simulation results are compared with the results obtained through the proposed analysis method. The simulated four port structure is shown in Figure 3.15. Identical slots have offset x_{off}, length l and the distance between them is d. During the analysis, d is varied from 70mm to 300mm.

By considering the symmetry of the structure, the active impedance is calculated from S-parameter data by using the following equations:

$$\frac{Z_1^a}{Z_0} = \frac{Z_2^a}{Z_0} = \frac{1}{2}\left(\frac{2R}{1-R} + \frac{2(1-T)}{T}\right) \tag{3.37}$$

where

$$\begin{aligned} R &= S_{11} + S_{13} \\ T &= S_{21} + S_{23} \end{aligned} \tag{3.38}$$

Active impedance of slots found by IE3D simulation is given in (3.37). Active impedance calculated by using the proposed analysis method is found by inserting related parameters into (3.35) and it becomes

$$\frac{Z_1^a}{Z_0} = \frac{Z_2^a}{Z_0} = \frac{f^2(x_{off}, l)}{\frac{f^2(x_{off}, l)}{Z/Z_0} + K_2 p_{12}}. \tag{3.39}$$

V_1^s / V_2^s in front of p_{12} drops because it is equal to unity since slots and their feeds are identical. Z is the self impedance value and it is extracted by slot characterization.

Analysis is done for different slot offsets. Slot lengths are chosen resonant at the related slot offset. Analysis results for slot offsets $x_{off} = 0$ mm, 3mm, 5mm and 8mm are presented in Figure 3.16, Figure 3.17, Figure 3.18 and Figure 3.19, respectively. In figures, it is seen that real parts of the active impedances converge to resonant self impedance and imaginary parts converge to zero as the distance between slots increase. This is an expected result because the effect of mutual coupling reduces as d increases and slots behave as if they are isolated. When simulation results and the results found through the analysis method proposed in this work are compared, a good agreement is observed especially for smaller offset values. The small amount of shift observed between simulation and calculation results might be attributed to the infinitesimally thin assumption of the slots in the proposed method.

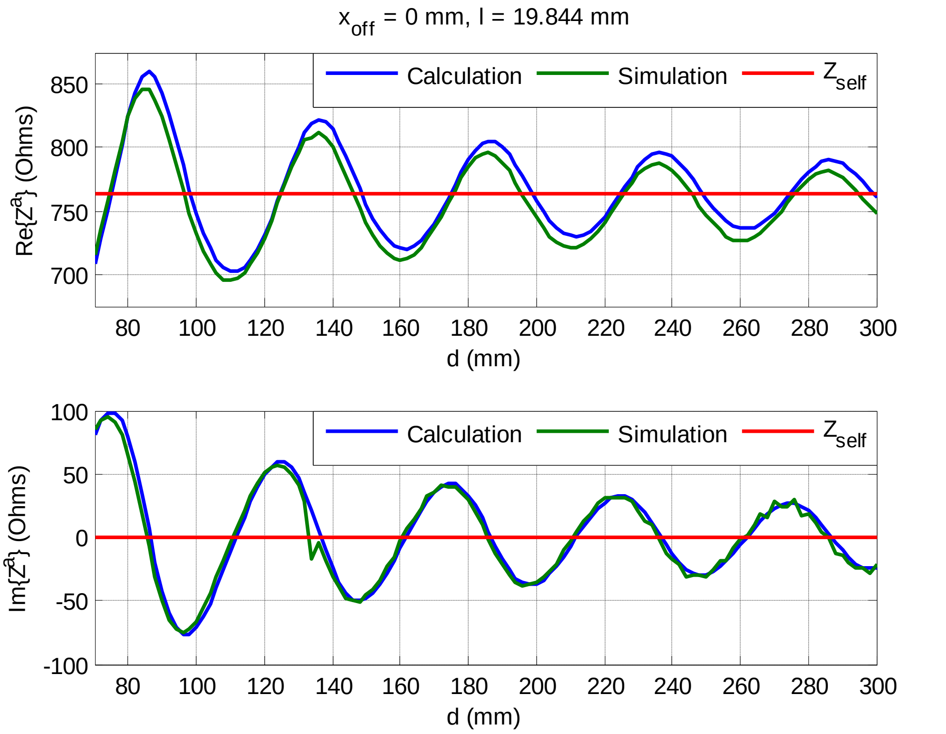

Figure 3.16: Active impedance Z^{a} vs. Distance d for x_{off} = 0 mm and l = 19.844 mm (Comparison of results found by offered analysis method and IE3D simulation)

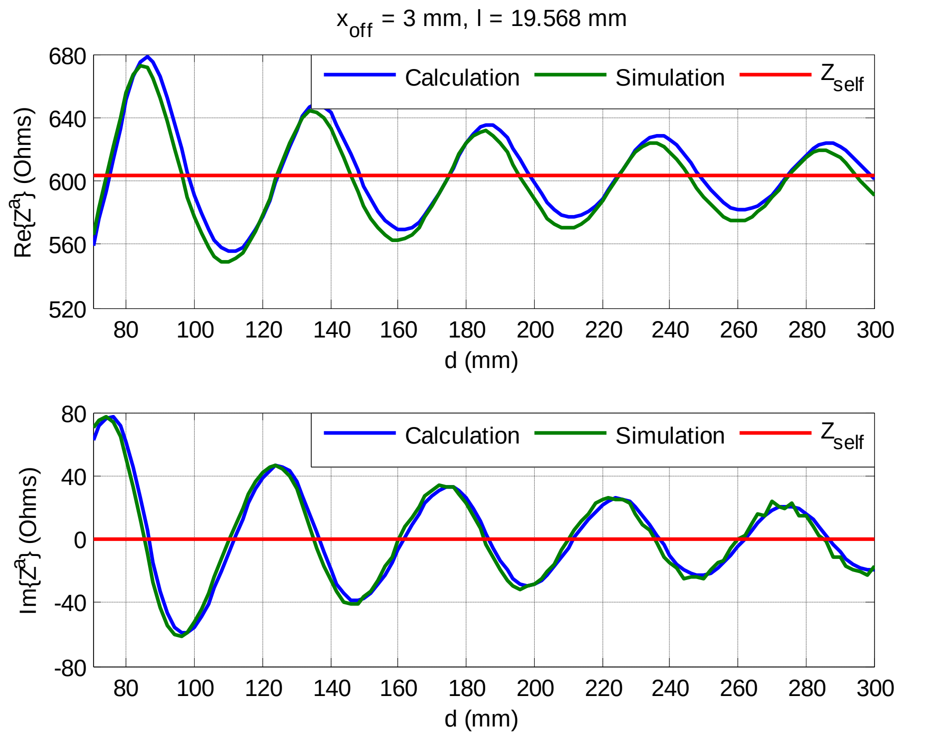

Figure 3.17: Active impedance Z^{a} vs. Distance d for x_{off} = 3 mm and l = 19.844 mm (Comparison of results found by offered analysis method and IE3D simulation)

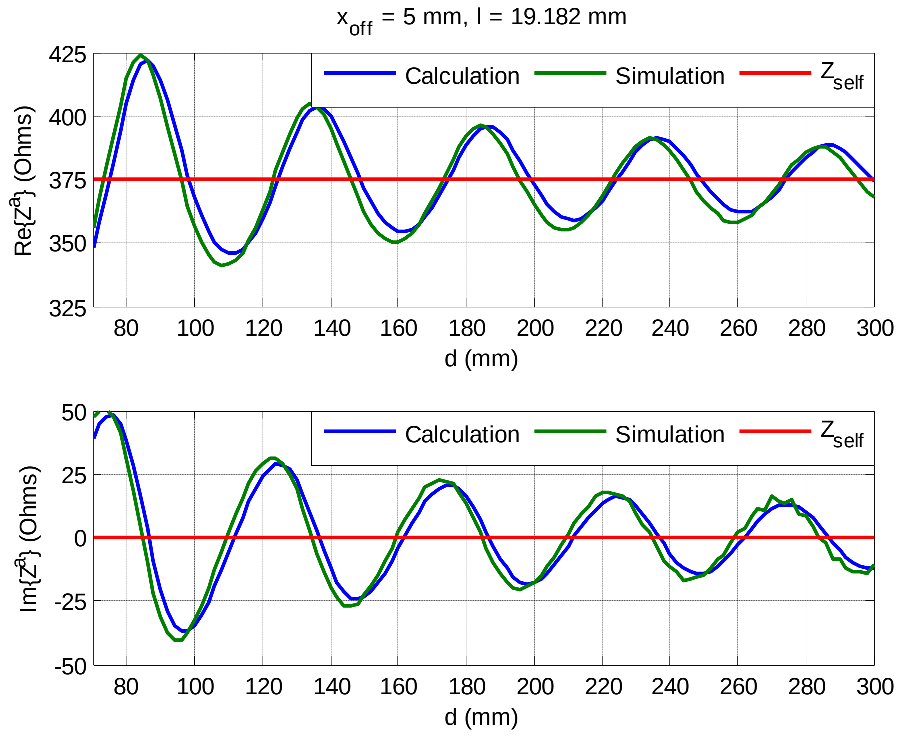

Figure 3.18: Active impedance Z^{a} vs. Distance d for x_{off} = 5 mm and l = 19.182 mm (Comparison of results found by offered analysis method and IE3D simulation)

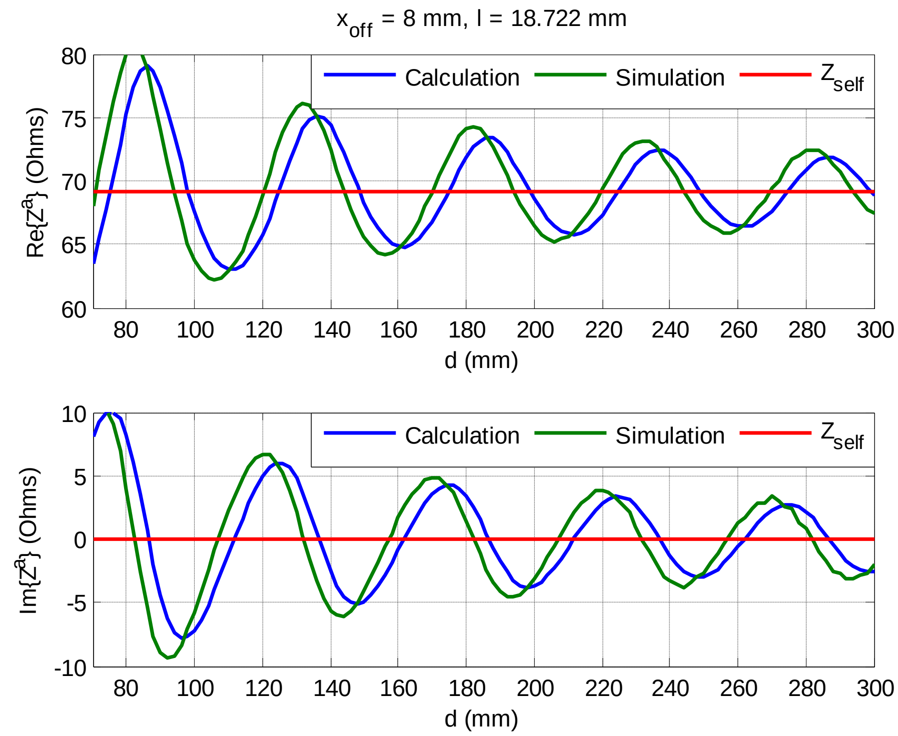

Figure 3.19: Active impedance Z^{a} vs. Distance d for x_{off} = 8 mm and l = 18.722 mm (Comparison of results found by offered analysis method and IE3D simulation)

Analysis of the two slot geometry gives reasonable results. As the next step, analysis can be extended to series-fed slot arrays like the traveling-wave array with 6 slots of which analysis and measurement results are given in Section 3.1. To analyze the array, the realized slot voltage values, that include the mutual coupling effects, are found by applying the fixed point iteration procedure to equations (3.34) and (3.35). This procedure is applied to analyze the 6 element array with parameters listed in Table 3.1. Steps of the analysis procedure, which can also be applied for other series arrays, are listed below:

i. Active impedance Z_n^a of each slot is calculated using (3.35) assuming that slot voltages are same as desired coefficients which are $\left|V^s\right| = $[0.8 0.9 1.0 1.0 0.9 0.8] with progressive phase shift of 270^o which can be expressed as $\angle V_n^s = n \times 270^o$. It is known that the actual slot voltage values will be different since the array is designed by ignoring mutual coupling effects. However, they are a suitable choice for initial coefficients to start the iterations. Since $(l_n, x_{off,n})$ couplets are fixed, self-impedance values Z_n's are constant.

ii. I_n at each slot node is calculated by making use of equation (3.3) with Z_n^a's calculated in the previous step.

iii. Combining equations (3.34) and (3.35) gives the equation below:

$$\frac{f_n I_n}{K_1} = \frac{f_n^2 V_n^s}{Z_n / Z_0} + K_2 \sum_{\substack{m=1 \\ m \neq n}}^{N} V_m^s p_{mn}. \tag{3.40}$$

Writing (3.40) in matrix form as it is done in [19] and solving it for V_n^s as below gives the new slot voltages.

$$\begin{bmatrix} V_1^s \\ V_2^s \\ \vdots \\ V_N^s \end{bmatrix} = \begin{bmatrix} \frac{f_1^2}{Z_1/Z_0} & K_2 p_{21} & \cdots & K_2 p_{N1} \\ K_2 p_{12} & \frac{f_2^2}{Z_2/Z_0} & & \\ \vdots & & \ddots & \\ K_2 p_{1N} & & & \frac{f_N^2}{Z_N/Z_0} \end{bmatrix}^{-1} \begin{bmatrix} I_1 f_1 \\ I_2 f_2 \\ \vdots \\ I_N f_N \end{bmatrix} \tag{3.41}$$

iv. V_n^s found in step (iii) are compared with the initial slot voltages assumed in the first step. If the change in slot voltages is in desired limits, realized slot voltages, according to the analysis including the mutual coupling, become these slot voltages. Otherwise, a new iteration is done starting from step (i) using the slot voltages found in step (iii) as the initial slot voltages. Iterations continue until the slot voltage converges to a value.

After completing the analysis for the antenna, realized slot voltages (array coefficients) are found as seen in Table 3.4. Since ratio of slot voltages between each other is important rather than the exact value, normalized values are shown in the table.

Table 3.4: Realized slot voltages found after analysis including mutual coupling for Linear Traveling-Wave MS-Fed Slot Array Antenna with 6 slots

	Desired		Realized	
Slot No.	|Vs|	Phase Prog. (deg.)	|Vs|	Phase Prog. (deg.)
1	0.8	-	0.800	-
2	0.9	+270	0.591	+295.6
3	1.0	+270	0.653	+273.3
4	1.0	+270	0.728	+269.8
5	0.9	+270	0.389	+264.7
6	0.8	+270	0.316	+283.8

Array factor is calculated with slot voltages that are found by offered analysis method and is compared with the desired array factor, measurement results and CST simulation results in Figure 3.20.

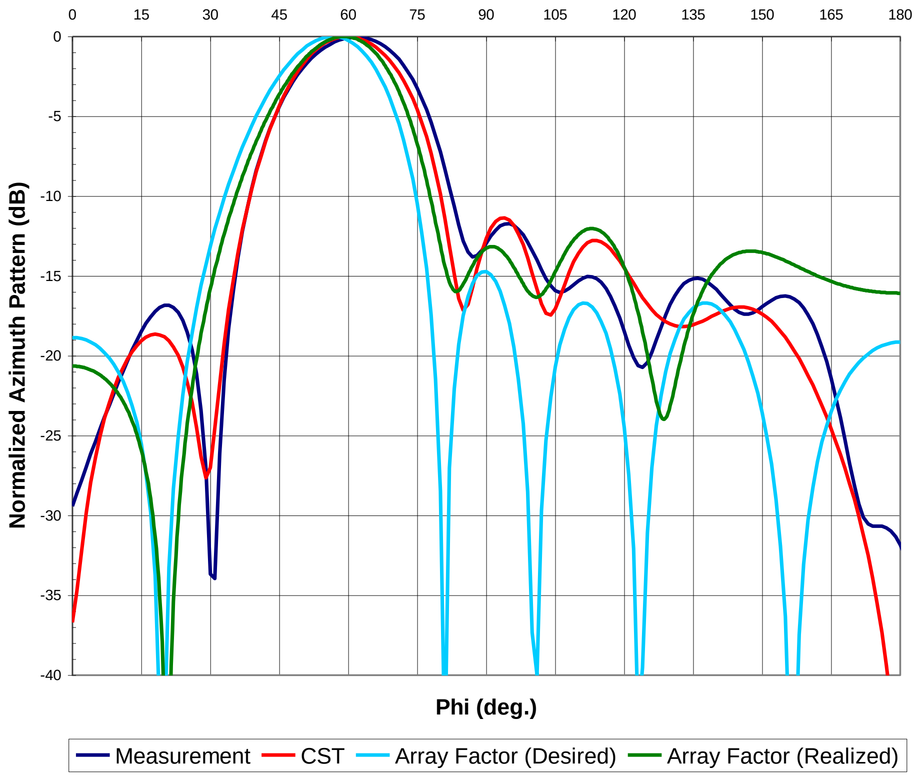

Figure 3.20: Normalized Azimuth Pattern of Linear Traveling-Wave MS-fed Slot Array Antenna (Comparison with array factor found by analysis including mutual coupling effects)

It would be better to remind that the array was designed by ignoring mutual coupling effects and an increase in the sidelobe levels and a shift in the beam direction was observed according to measurement and simulation results. It is seen that by using the proposed analysis method that includes mutual coupling effects, the shift in the direction of the main beam and the increase in the sidelobe levels can be predicted to some extend. However, there are some discrepancies between simulation results and the results obtained by the proposed analysis method. It is thought that this discrepancy might be due to the different models assumed for the ground plane and the dielectric substrate in the simulations and in the proposed method. In the proposed analysis method, it is assumed that slots lie on an infinite grounded dielectric slab. However, the ground plane of the measured antenna ends at a distance nearly half wavelength away from the slots. In CST simulations, the size of the substrate and the ground plane are the same as the size of the manufactured antenna. In order to decide whether the discrepancy between the simulation results and the results obtained by the proposed method is due to the finite ground plane size, the manufactured antenna is also simulated with an infinite ground plane and infinite substrate using IE3D. Results of this analysis are shown in Figure 3.21. It is seen that pattern obtained by full-wave analysis of IE3D and obtained by realized slot voltages agree well in the first sidelobe level and shift in the main beam direction. Beam shapes obtained by two methods are similar. Hence, it can be concluded that although the proposed method is successful in predicting the radiation pattern of the array by incorporating the mutual coupling effects, the accuracy of the method can be improved by considering the size of the ground plane and the dielectric substrate. This can be a research topic for future studies.

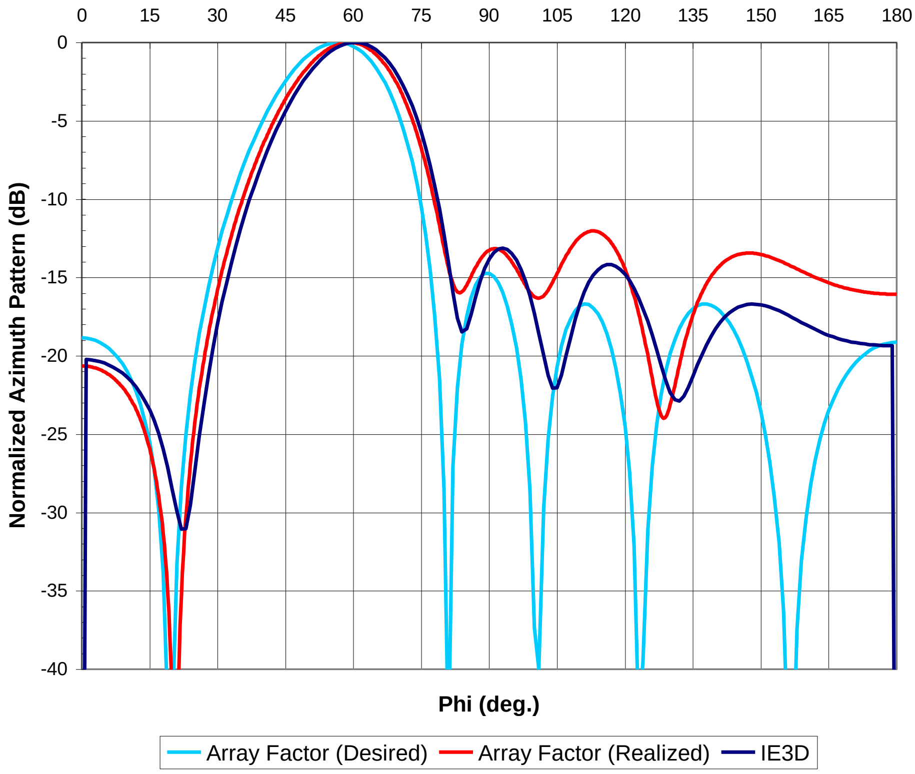

Figure 3.21: Normalized Azimuth Pattern of Linear Traveling-Wave MS-fed Slot Array Antenna (Comparison of array factor found by analysis including mutual coupling effects and simulation results with infinite ground plane obtained by IE3D)

Antennas of which slot parameters and excitation coefficients are given in Table 3.2 and Table 3.3 are also analyzed using the offered method. Realized excitation coefficients for the antenna in Table 3.2 is seen in Table 3.5 and the array factor with these coefficients are compared with the pattern simulated by IE3D in Figure 3.22. As seen in the figure, a good agreement with the full-wave analysis results is obtained for this antenna as well, especially for the characteristics of the main lobe and for the sidelobe levels.

Table 3.5: Realized slot voltages found after analysis including mutual coupling for Linear Traveling-Wave MS-Fed Slot Array Antenna with 6 slots synthesized with $Z_1/Z_0=3$ for 15 dB sidelobe level

	Desired		Realized	
Slot No.	|Vs|	Phase Prog. (deg.)	|Vs|	Phase Prog. (deg.)
1	0.8	-	0.800	-
2	0.9	+270	0.673	+302.0
3	1.0	+270	0.615	+270.4
4	1.0	+270	0.789	+273.9
5	0.9	+270	0.359	+260.9
6	0.8	+270	0.350	+289.2

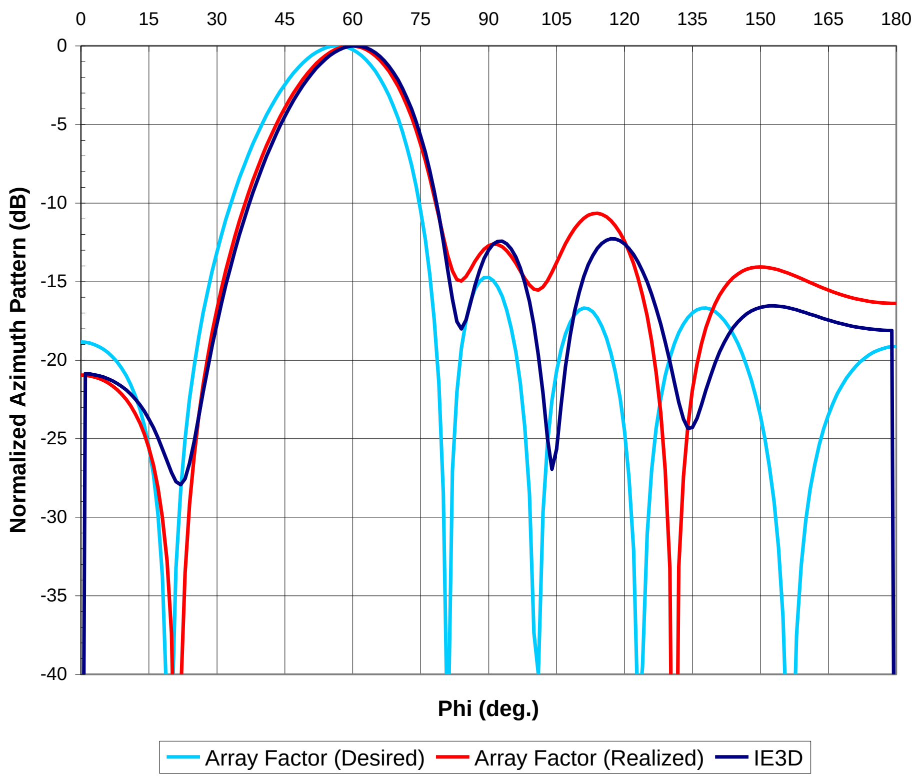

Figure 3.22: Normalized Azimuth Pattern of Linear Traveling-Wave MS-fed Slot Array Antenna synthesized with Z_1/Z_0=3 for 15 dB sidelobe level. (Comparison of array factor found by analysis including mutual coupling effects and simulation results with infinite ground plane obtained by IE3D)

Finally in Figure 3.23, pattern of the antenna with realized array coefficients given in Table 3.6 is shown and it is seen that agreement in the main lobe is achieved again.

After analysis of series arrays, it is seen that analysis method developed by modeling series impedances as active impedance gives reasonable results for slot voltages although several assumptions were made. Derived equations given by (3.34) and (3.35) can be used to design microstrip line fed slot arrays by considering the mutual coupling effects.

Table 3.6: Realized slot voltages found after analysis including mutual coupling for Linear Traveling-Wave MS-Fed Slot Array Antenna with 6 slots synthesized with Z_1/Z_0=3 for 20 dB sidelobe level

	Desired		Realized	
Slot No.	|Vs|	Phase Prog. (deg.)	|Vs|	Phase Prog. (deg.)
1	0.55	-	0.550	-
2	0.78	+270	0.632	+293.8
3	1.00	+270	0.554	+280.0
4	1.00	+270	0.627	+276.5
5	0.78	+270	0.262	+267.6
6	0.55	+270	0.204	+288.0

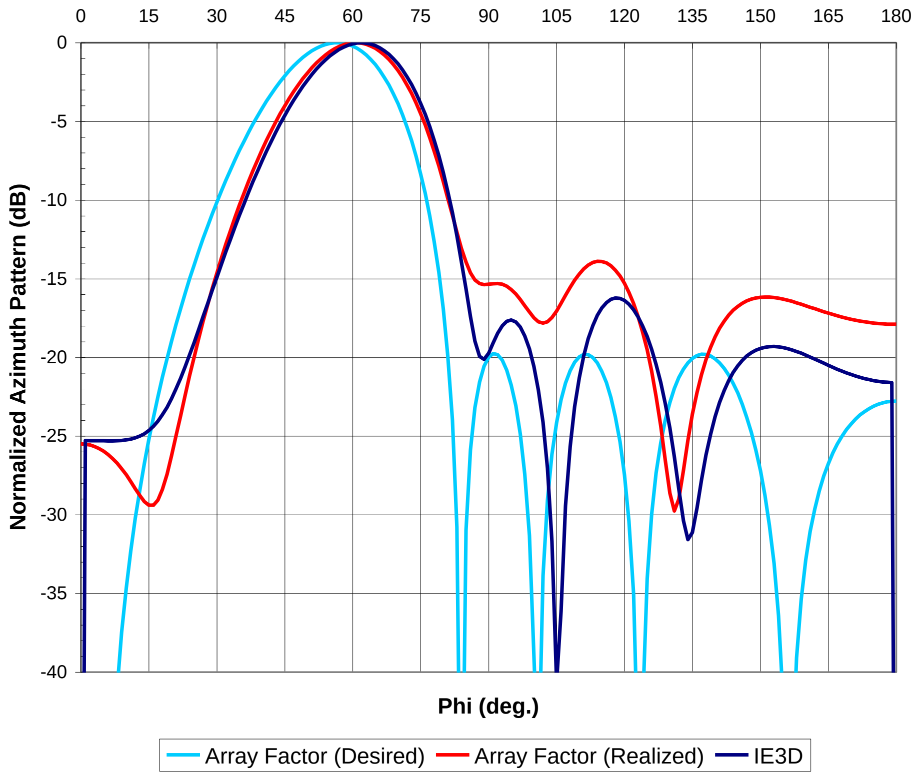

Figure 3.23: Normalized Azimuth Pattern of Linear Traveling-Wave MS-fed Slot Array Antenna synthesized with Z_1/Z_0=3 for 20 dB sidelobe level. (Comparison of array factor found by analysis including mutual coupling effects and simulation results with infinite ground plane obtained by IE3D)

CHAPTER 4

CONCLUSIONS

Linear arrays of microstrip-fed transverse slot antennas are investigated in this thesis. Since they are low profile structures that can be easily manufactured with low cost and easily integrated with other microwave circuitry, they are good candidates for use in array applications that do not require high power levels.

In this thesis, series arrays of microstrip-fed slots are designed by using the method offered in [11] and one of these arrays is manufactured. In this design method, array of slots is modeled by an equivalent circuit model in which the slots are modeled by series impedances. However, this series impedance model is constructed by ignoring the mutual coupling between the slots. Full-wave analysis results of designed arrays and measurements done on the manufactured array show that the desired performance is not satisfied. To reach the desired performance, it is needed to model mutual coupling effects in the equivalent circuit model. However, no such a design method that encounters for mutual coupling effects exists in literature. For the design of waveguide-fed and stripline-fed slot arrays, a design method including mutual coupling effects into the equivalent circuit model is reported by Elliott [12]-[15]. In Elliott's studies results of a similar analysis done by Pozar [7] for microstrip-fed slots is done for waveguide-fed and strip-line fed slots and mutual coupling effects are included into the equivalent circuit model by developing the active impedance model.

Investigating Elliott's work gives the motive for incorporating equivalent circuit model in [11] and results of analysis of microstrip-fed in [7] as Elliott has done for other feeding structures. In this thesis, expressions for the active impedance model of a transverse microstrip-fed slot antenna array are derived, and the designed arrays are analyzed by using these expressions. Comparing the results of the proposed analysis method with the EM simulation and measurement results, it is concluded that by including the mutual coupling effects into the equivalent circuit model, the main beam direction and the sidelobe level of the designed antenna are calculated with improved accuracy. The accuracy of the proposed method could be further improved by incorporating the effects of finite ground plane size into the formulation.

Expressions developed in this thesis can also be used for the design of microstrip-fed slot arrays by combining the proposed analysis method with a non-linear optimization method as done by Elliott to design slotted waveguide arrays. It is considered that design by making use of these equations will meet desired performance. As a future work, design of arrays will be realized by this analysis method incorporating mutual coupling effects and equivalent circuit model

REFERENCES

[1] Elliott, R.S. & Kurtz, L.A., "The design of small slot arrays", *IEEE Transactions on Antennas and Propagation*, vol. AP-26, pp. 214-219, March 1978.

[2] Elliott, R.S., Antenna Theory and Design, IEEE Press, New Jersey, 2003.

[3] Wang W., Zhong, S., Zhang Y. & Liang X., "A broadband slotted ridge waveguide antenna array", *IEEE Transactions on Antennas and Propagation*, vol. 54, no. 8, pp. 2416-2420, August 2006.

[4] Coetzee, J.C., Joubert J. & Tan, W.L., "Frequency performance enhancement of resonant slotted waveguide arrays through the use of wideband slot radiators or subarraying", *Microwave and Optical Technology Letters*, vol. 22, no.1, pp. 35-39, July 1999.

[5] Yoshimura, Y., "A microstripline slot antenna", *IEEE Transactions on Microwave Theory and Techniques*, vol. 20, pp. 760-762, November 1972.

[6] Das, B.N. & Joshi, K.K., "Impedance of a radiating slot in the ground plane of a microstrip line", *IEEE Transactions on Antennas and Propagation*, vol. AP-30, no. 5, pp. 922-926, March 1982.

[7] Pozar, D., "A reciprocity method of analysis for printed slots and slot-coupled microstrip antennas", *IEEE Transactions on Antennas and Propagation*, vol. 34, no. 12, pp. 1439-1446, December 1986.

[8] Akhavan, H.G. & Mirshekar-Syakhal, D., "Approximate model for microstrip fed slot antennas", *Electronics Letters*, vol. 30, no. 23, pp. 1902-1903, November 1994.

[9] Kim, J.P. & Park, W.S., "Network modeling of an inclined and off-center microstrip-fed slot antenna", *IEEE Transactions on Antennas and Propagation*, vol. 46, no. 8, pp. 1182-1188, August 1998.

[10] Zhu, L. & Wu, K., "Complete circuit model of microstrip-fed slot radiator: Theory and experiments", *IEEE Microwave and Guided Wave Letters*, vol. 9, no. 8, pp. 305-307, August 1999.

[11] Tulintseff, A.N., "Series-fed type linear arrays of dipole and slot elements transversely coupled to a microstrip line", *Proceedings of the IEEE Antennas and Propagation Society Int. Symp.*, vol. 1, pp. 128-131, June 1993.

[12] Elliott, R.S., "An improved design procedure for small arrays of shunt slots", *IEEE Transactions on Antennas and Propagation*, vol. AP-31, no. 1, pp. 48-53, January 1983.

[13] Elliott, R.S., "Design of waveguide-fed series slot arrays", *IEE Proceedings*, vol. 129, pt. H, no. 4, pp. 165-169, August 1982.

[14] Shavit, R. & Elliott, R.S., "Design of transverse slot arrays fed by a boxed stripline", *IEEE Transactions on Antennas and Propagation*, vol. AP-31, no. 4, pp. 545-552, July 1983.

[15] Park, K.P. & Elliott, R.S., "Design of collinear longitudinal slot arrays fed by boxed stripline", *IEEE Transactions on Antennas and Propagation*, vol. AP-29, no. 1, pp. 135-139, July 1981.

[16] Aksun, M.I., "A robust approach for the derivation of closed-form Green's functions", *IEEE Transactions on Microwave Theory and Techniques*, vol. 44, no. 5, pp. 651-658, May 1996.

[17] McNamara, D.A & Joubert J., "Experimentally determined equivalent network scattering parameters for edge slots in rectangular waveguide for use as reference data", *IEEE Microwave and Guided Wave Letters*, vol. 3, pp. 405-407, November 1993.

[18] Aksun, M.I., "A robust approach for the derivation of closed-form Green's functions", *IEEE Transactions on Microwave Theory and Techniques*, vol. 44, no. 5, pp. 651-658, May 1996.

[19] Elliott, R.S., "On the design of traveling-wave-fed longitudinal shunt slot arrays", *IEEE Transactions on Antennas and Propagation*, vol. 27, no. 5, pp. 717-720, September 1979.

APPENDIX A

GREEN'S FUNCTIONS

Green's function components for grounded dielectric slab are listed below [7].

G_{xx}^{EJ} : E_x at (x, y, d) due to a unit $\hat{x}$ directed electric current element at (x_0, y_0, d)

G_{yx}^{HJ} : H_y at $(x, y, 0)$ due to a unit $\hat{x}$ directed electric current element at (x_0, y_0, d)

G_{yy}^{HM} : H_y at $(x, y, 0)$ due to a unit $\hat{y}$ directed magnetic current element at $(x_0, y_0, 0)$

G_{xy}^{EM} : E_x at (x, y, d) due to a unit $\hat{y}$ directed magnetic current element at $(x_0, y_0, 0)$

Spectral domain Green's functions $\tilde{G}$ are defined as Fourier transform of G as

$$G(x,y) = \frac{1}{4\pi^2}\int_{-\infty}^{\infty}\int_{-\infty}^{\infty}\tilde{G}(k_x,k_y)e^{jk_x(x-x_0)}e^{jk_y(y-y_0)}dk_x dk_y. \tag{A.1}$$

Then,

$$\tilde{G}_{xx}^{EJ} = \frac{j\eta_0}{k_0}\frac{(\varepsilon_r k_0^2 - k_x^2)k_z \cos k_1 d + jk_1(k_0^2 - k_x^2)\sin k_1 d}{T_e\, T_m}\sin k_1 d \tag{A.2}$$

$$\tilde{G}_{yx}^{HJ} = \frac{-jk_x^2(\varepsilon_r - 1)\sin k_1 d}{T_e\, T_m} + \frac{k_1}{T_e} \tag{A.3}$$

$$\tilde{G}_{yy}^{HM} = \frac{-j}{k_0\eta_0}\left[\frac{j(k_1\cos k_1 d + jk_2\varepsilon_r \sin k_1 d)(\varepsilon_r k_0^2 - k_y^2)}{k_1 T_m} - \frac{jk_y^2 k_1(\varepsilon_r - 1)}{T_e\, T_m}\frac{(k_0^2 - k_y^2)}{jk_2}\right] \tag{A.4}$$

$$\tilde{G}_{xy}^{EM} = -\tilde{G}_{yx}^{HJ} \tag{A.5}$$

where

$$T_e = k_1 \cos k_1 d + jk_2 \sin k_1 d$$

$$T_m = \varepsilon_r k_2 \cos k_1 d + jk_1 \sin k_1 d$$

$$k_1^2 = \varepsilon_r k_0^2 - \beta^2, \quad \mathrm{Im}\, k_1 < 0$$

$$k_2^2 = k_0^2 - \beta^2, \quad \mathrm{Im}\, k_2 < 0$$

$$\beta^2 = k_x^2 + k_y^2$$

$$k_0^2 = \omega^2 \mu_0 \varepsilon_0 = (2\pi / \lambda_0)^2$$

$$\mu_0 = \sqrt{\mu_0 / \varepsilon_0}.$$

Microstrip line field H_y is written by assuming uniform current distribution along width as

$$H_y(x, y) = \frac{1}{2\pi} \int_{-\infty}^{\infty} F_u(k_y) \tilde{G}_{yx}^{HJ}(k_x = -\beta, k_y) e^{-j\beta x} e^{jk_y y} dk_y \tag{A.6}$$

where $F_u(k_y)$ is the Fourier transform of the uniform current distribution $f_u(y)$ over line width W.

$$F_u(k_y) = \frac{\sin k_y W / 2}{k_y W / 2} \tag{A.7}$$

$$f_u(y) = \begin{cases} 1/W, & for\ |y| < W/2 \\ 0, & for\ |y| > W/2 \end{cases} \tag{A.8}$$

Normalized field modal field component is $h_y = H_y / \sqrt{Z_0}$ according to condition is (3.11).